

ARMY RESEARCH LABORATORY



**Design of Experiments Study of the Initial
Extended Area Protection and Survivability
(EAPS) Projectile System**

by Michael M. Chen

ARL-TR-4109

May 2007

NOTICES

Disclaimers

The findings in this report are not to be construed as an official Department of the Army position unless so designated by other authorized documents.

Citation of manufacturer's or trade names does not constitute an official endorsement or approval of the use thereof.

DESTRUCTION NOTICE—Destroy this report when it is no longer needed. Do not return it to the originator.

Army Research Laboratory

Aberdeen Proving Ground, MD 21005-5066

ARL-TR-4109

May 2007

Design of Experiments Study of the Initial Extended Area Protection and Survivability (EAPS) Projectile System

Michael M. Chen

Weapons and Materials Research Directorate, ARL

REPORT DOCUMENTATION PAGE			Form Approved OMB No. 0704-0188		
Public reporting burden for this collection of information is estimated to average 1 hour per response, including the time for reviewing instructions, searching existing data sources, gathering and maintaining the data needed, and completing and reviewing the collection information. Send comments regarding this burden estimate or any other aspect of this collection of information, including suggestions for reducing the burden, to Department of Defense, Washington Headquarters Services, Directorate for Information Operations and Reports (0704-0188), 1215 Jefferson Davis Highway, Suite 1204, Arlington, VA 22202-4302. Respondents should be aware that notwithstanding any other provision of law, no person shall be subject to any penalty for failing to comply with a collection of information if it does not display a currently valid OMB control number. PLEASE DO NOT RETURN YOUR FORM TO THE ABOVE ADDRESS.					
1. REPORT DATE (DD-MM-YYYY) May 2007		2. REPORT TYPE Final		3. DATES COVERED (From - To) July 2006 through February 2007	
4. TITLE AND SUBTITLE Design of Experiments Study of the Initial Extended Area Protection and Survivability (EAPS) Projectile System			5a. CONTRACT NUMBER		
			5b. GRANT NUMBER		
			5c. PROGRAM ELEMENT NUMBER		
6. AUTHOR(S) Michael M. Chen (ARL)			5d. PROJECT NUMBER 622618.H80		
			5e. TASK NUMBER		
			5f. WORK UNIT NUMBER		
7. PERFORMING ORGANIZATION NAME(S) AND ADDRESS(ES) U.S. Army Research Laboratory Weapons and Materials Research Directorate Aberdeen Proving Ground, MD 21005-5066			8. PERFORMING ORGANIZATION REPORT NUMBER ARL-TR-4109		
9. SPONSORING/MONITORING AGENCY NAME(S) AND ADDRESS(ES)			10. SPONSOR/MONITOR'S ACRONYM(S)		
			11. SPONSOR/MONITOR'S REPORT NUMBER(S)		
12. DISTRIBUTION/AVAILABILITY STATEMENT Approved for public release; distribution is unlimited.					
13. SUPPLEMENTARY NOTES					
14. ABSTRACT A novel approach is proposed for assessing the effects of gun barrel centerline variations on Extended Area Protection and Survivability (EAPS) projectile launch dynamics. The technique of experiment design was adopted to simulate an array of deformed gun tubes representing reasonable manufacturing tolerance. Subsequently, in-bore structural analysis of the EAPS projectile system subject to the simulated gun barrels was performed. The projectile responses including transitional and rotational velocities at the muzzle were obtained. The analysis of variance method was then used to identify the sources of variability and to determine the significance of each gun shape. Based on the response statistics, no erratic launch conditions should be expected for the EAPS projectile because of normal barrel centerline variations.					
15. SUBJECT TERMS barrel centerline variation; EAPS projectile; in-bore dynamics; 60-mm projectile					
16. SECURITY CLASSIFICATION OF:			17. LIMITATION OF ABSTRACT SAR	18. NUMBER OF PAGES 38	19a. NAME OF RESPONSIBLE PERSON Michael M. Chen
a. REPORT Unclassified	b. ABSTRACT Unclassified	c. THIS PAGE Unclassified			19b. TELEPHONE NUMBER (Include area code) 410-278-6146

Contents

List of Figures	iv
List of Tables	iv
Acknowledgments	v
1. Introduction	1
2. Projectile Description and Modeling	2
3. Design of Experiments	4
4. Analysis of Variance	6
5. Response Statistics	13
6. Summary	14
7. References	17
Appendix A. List of Lateral Displacement (millimeters) for the Level Combination of Four Barrel Shape Variables in DOE Design	19
Appendix B. Response Values of Translational Velocity (millimeters per second) at the Muzzle From DOE Analysis	21
Appendix C. Response Values of Yaw Angle (degrees) and Yaw Rate (degrees per second) at the Muzzle From DOE Analysis	18
Appendix D. Response Values of Pitch Angle (degrees) and Pitch Rate (degrees per second) at the Muzzle From DOE Analysis	25
Appendix E. Muzzle Yaw Rate Response Surface Model	27
Distribution List	29

List of Figures

Figure 1. Geometry of the initial EAPS projectile.....	2
Figure 2. Material configuration of the initial EAPS projectile.....	3
Figure 3. Time history of in-bore base pressure.	3
Figure 4. Simplified configuration of the initial EAPS finite element model.	4
Figure 5. Display of four fundamental deflection shapes of a gun barrel.....	5
Figure 6. Comparison of contributing percentage of four barrel shapes and their interactions with (a) axial velocity, (b) lateral velocity, and (c) vertical velocity.....	8
Figure 7. Comparison of contributing percentage of four barrel shapes and their interactions with (a) yaw angle and (b) pitch angle.....	9
Figure 8. Comparison of contributing percentage of four barrel shapes and their interactions with (a) yaw rate and (b) pitch rate.....	10
Figure 9. Residual plots of projectile (a) X, (b) Y, and (c) Z velocities at the muzzle.....	11
Figure 10. Residual plots of projectile (a) yaw rate and (b) pitch rate at the muzzle.....	12
Figure 11. Changes in (a) X, (b) Y, and (c) Z velocities by a change in the levels of the four barrel shapes.....	15

List of Tables

Table 1. Absolute lateral displacement (mm) of a gun barrel at five chosen sections.	6
Table 2. Response statistics of projectile translational velocity at the muzzle from DOE analysis.....	13
Table 3. Response statistics of projectile rotational angle and rotational rate at the muzzle from DOE analysis.....	13

Acknowledgments

The author wishes to thank Dr. Peter Plostins, program manager of the Extended Area Protection and Survivability (EAPS) project, for his financial support for the study. The author highly appreciates the many valuable suggestions provided by Mr. Bernard Guidos of the U.S. Army Research Laboratory (ARL) through technical review. In addition, the author is grateful for gun barrel centerline variations data given by Dr. Mark Bundy of ARL. This work was supported in part by a grant of high-performance computing time from the U.S. Department of Defense High Performance Computing Modernization program at ARL's Major Shared Resource Center, Aberdeen Proving Ground, Maryland.

INTENTIONALLY LEFT BLANK

1. Introduction

The U.S. Army Research Laboratory (ARL) supports a program named Extended Area Protection and Survivability (EAPS) and led by the Aviation and Missile Research Development and Engineering Center, whose mission is to investigate guided ammunition technologies to defend the battle space against any presented targets. Specifically, the objective of the program is to develop and demonstrate critical supporting technologies, including interceptor, sensor, and fire controls, to enable stationary and mobile 360-degree hemispherical extended area protection from direct and indirect fires. Preliminary structural design and analysis of an initial EAPS projectile system has been performed by Chen (*1, 2*) to ensure that the structural integrity is maintained during launch. Since the guided ammunition system was designed to hit and destroy hostile objects (such as mortars, rockets, and artillery), the whole process must be undertaken with high accuracy at an extended range in a very short period of time frame. Nevertheless, a variety of uncertain factors that may influence overall performance of the projectile system exist at any stage of the launch process, starting from primer ignition, propellant combustion, projectile in-bore travel, and free-body flight throughout target hitting. The uncertainties must be studied and taken into account when one is designing a highly reliable weapon system such as EAPS ammunition system.

Muzzle responses including translational and rotational responses are important indicators for gun-projectile performance. However, because of various uncontrollable factors, it has not been easy to obtain repeatable muzzle responses from many experimental tests. As a result, understanding the contributing factors to the variations of muzzle responses and the sensitivity of the responses to the random factors is essential when one is evaluating the reliability of an ammunition system. In the past decade, a few studies to identify and quantify variables that may affect muzzle velocity have been conducted by researchers (*3 through 5*). In previous investigations, the sensitivity of muzzle responses to a large number of random variables associated with a projectile system has been evaluated. Although the interior ballistic modeling in the literature was quite comprehensive, it did not cover gun barrel centerline variations that have been known to significantly influence in-bore projectile behavior. Thus, Erlin (*6*) analyzed a number of hypothetical cases when a gun barrel centerline changed from a bent state to an unbent state and found that lateral loads could be dramatically amplified by a small sine wave in a gun barrel centerline. In addition, Bundy et al. (*7, 8*) assessed the interactions between tank motion and gun barrel rotation and translation by enumerating the ten most likely barrel shape combinations for the evaluation of gun accuracy. Furthermore, Newill et al. (*9*) explored the sensitivity of jump errors relative to gun tube centerline shapes and determined the optimal centerline shape for best accuracy performance.

Since gun barrel centerline plays an important role in interior ballistic analysis, this report proposes a novel approach to assessing the effects of deformed gun tubes on projectile launch dynamics. Instead of using one or some measured barrel centerline data for the analysis, a more comprehensive study that considers stochastic characteristics of gun tube centerline was conducted, which is

more realistic of the fact that the centerlines of the gun barrels used by Soldiers at war fields deviated substantially because of the variations of combat environment and situations. Consequently, a large number of distinct barrel shapes for the analysis of EAPS projectile system were schematically simulated through design of experiments (DOE) techniques. In-bore dynamic analyses with the array of deformed gun barrels were then conducted, and the results were statistically evaluated and discussed.

2. Projectile Description and Modeling

The topology of the initial EAPS projectile was outlined with the PRODAS (PROjectile Design and Analysis System) tool, which was based on gun barrel specifications and certain aerodynamic characteristics. According to the prototype, a three-dimensional solid model was created, as shown in figure 1. The initial EAPS projectile was equipped with a windscreen and a penetrator in the front, which had an ogive length and radius of 70.5 mm and 1380 mm, respectively. Four fins for stabilization had a fin span of 50 mm. The length of the projectile from nose to tail was 317 mm. An outer diameter of 23.5 mm was used for this study. The inside of its body was divided into two cavity areas. The forward cavity may carry high explosive payload while the rear cavity was designed to accommodate electronic equipment. Overall speaking, the launch package consisted of projectile body, penetrator, windscreen, electronics, fins and sabot. The material configuration of the projectile system is illustrated in figure 2. The detailed physical and mechanical properties of the material for each component are presented in a previous report (1).

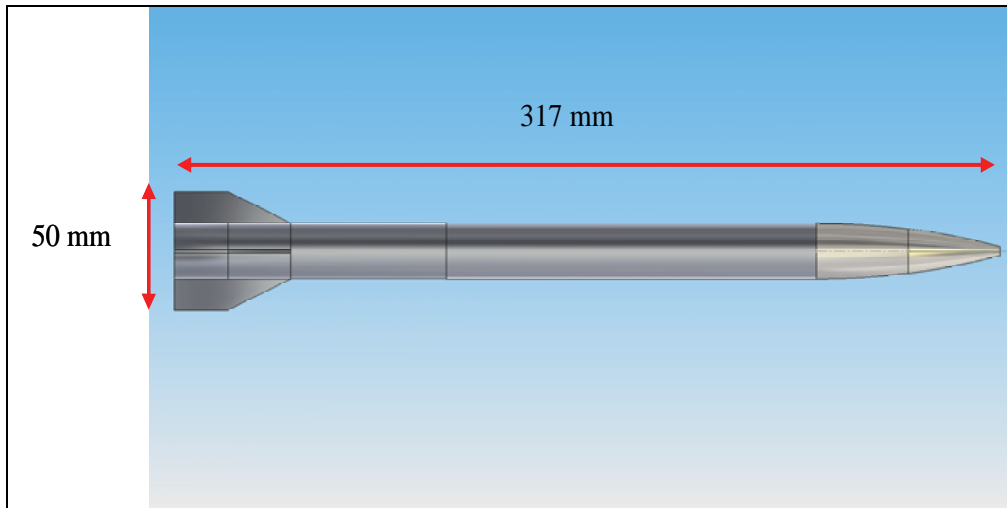


Figure 1. Geometry of the initial EAPS projectile.

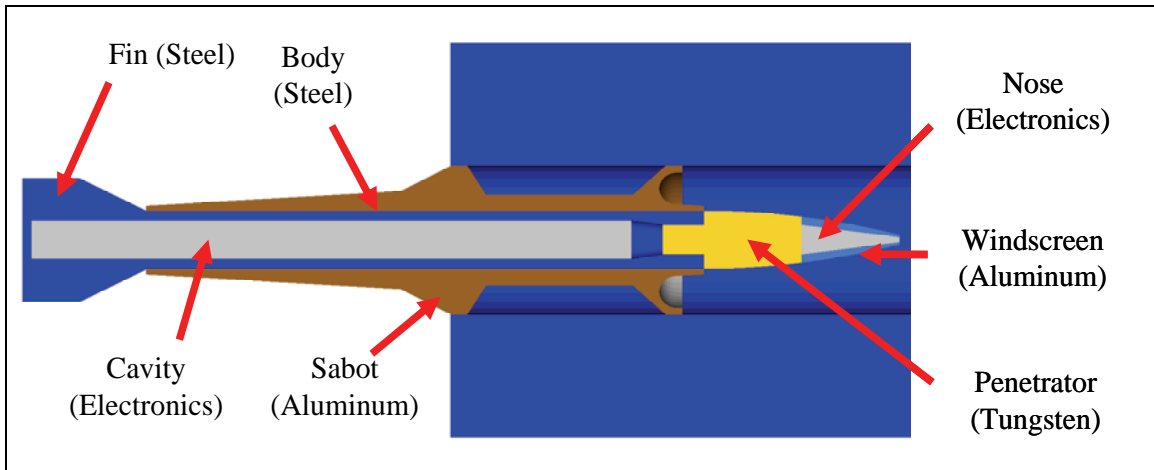


Figure 2. Material configuration of the initial EAPS projectile.

A 64-caliber smooth bore gun tube with an inner diameter of 60 mm and a total length of 3840 mm was used to simulate the projectile firing. M2 propellants with geometry of seven perforation grains were used for the propulsion. Considering a chamber volume of 1.3 liters, a base pressure-time curve was derived from IBHVG2 (interior ballistics of high velocity guns, version 2) and is shown in figure 3. The pressure curve exhibits a total duration of 5 ms and a peak value of 335 MPa taking place at 2.1 ms from the start of ignition.

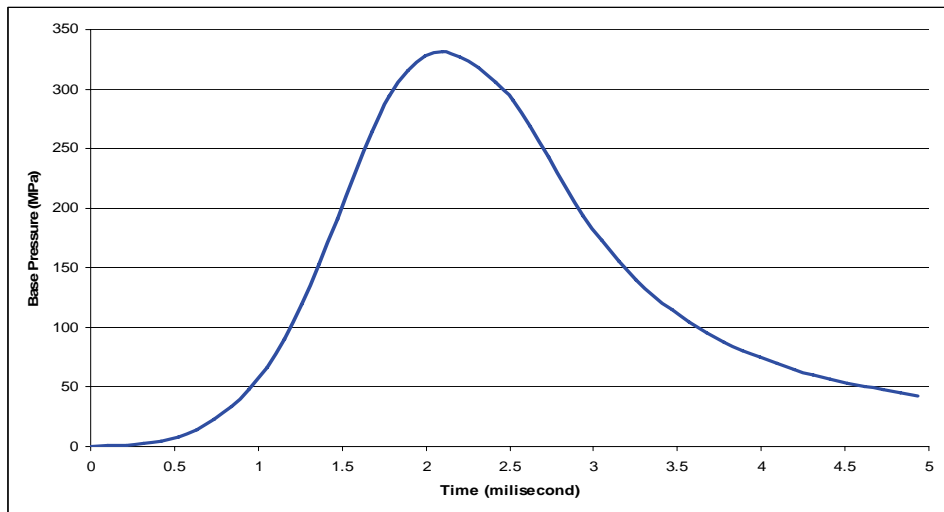


Figure 3. Time history of in-bore base pressure.

For computational efficiency in DOE analysis, the windscreen and stabilized fins were substituted with equivalent weight into their respective neighbor component so that the center of gravity (CG) of the projectile system remained at the same location. In addition, the weight of the sabot component was optimized, which reduced the total mass of the launch system to approximately 1 kg. The simplified projectile configuration and grids are displayed in figure 4. This model contained eight-node solid hexahedral elements. The total number of nodes and elements for the projectile

system were 53,761 and 42,984, respectively. Note that no tolerance in the diameter of the bore riders was modeled for the statistical simulation. Surface-to-surface contact elements were used for the interface with the gun barrel. Because the primary focus of the study was the effects of barrel flexure on muzzle responses, the rigid body responses of the projectile at the exit were used for the comparison.

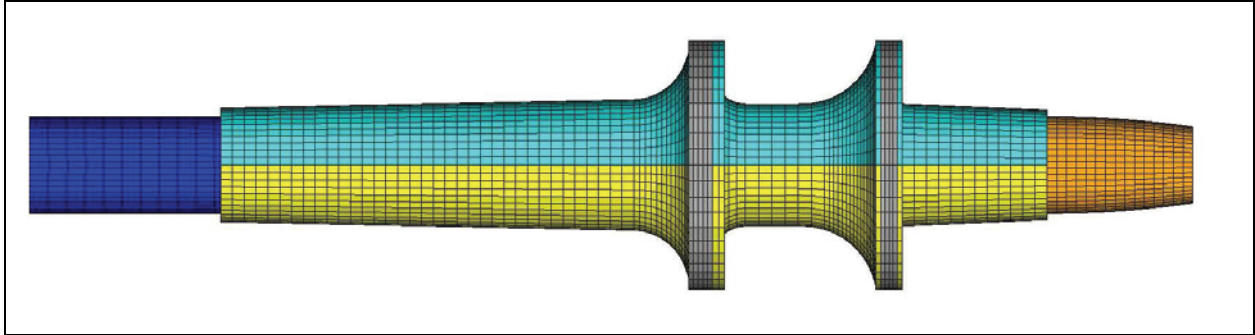


Figure 4. Simplified configuration of the initial EAPS finite element model.

3. Design of Experiments

Generally speaking, the centerline variations of a gun barrel may be attributed to a number of factors, such as manufacturing errors, uneven cooling, non-uniform wall thickness/erosion, vibrations, etc. Regardless of the sources of the variations, four fundamental barrel shapes were created and are shown in figure 5. Any combination of these four barrel shapes may account for the centerline variations because of one or more of the factors. Note that the displayed shapes have been magnified for visibility.

The steps to generate the barrel shapes can be described as follow:

- The gun barrel was equally divided into four areas, which generated five cross sections named A (muzzle), B, C, D, and E (breech);
- All the nodes of section E (i.e., at the breech area) were completely restrained, and the nodes of the other four sections were to be displaced only laterally (Y direction);
- All the nodes of section A were first displaced one unit while the other sections were all fixed, which yielded shape 1 variable. Note that a second order biasing factor was used for the “morphing” so that the continuity of the slope could hold.
- The third step was repeated for the nodes at the other three sections B, C, and D, which led to the generation of shapes 2, 3, and 4, respectively. The ranges of absolute lateral displacements along down-bore distance for these five sections are summarized in table 1 in which the numbers in the parentheses represent the ratio to the total length of the barrel. The magnitude of the dis-

placements was determined based on the characteristics of ten most likely barrel shapes proposed by Bundy et al. (8). Because the nodes of sections A and B exhibit higher deviations in the profile, a total of five levels was assigned as opposed to only three levels for the nodes of sections C and D. Note that the choices of the numbers of factors and levels were determined by the flexed barrel profile from a total of 37 cases concluded by Bundy et al. (8). The combination of the levels of the factors should constitute a good representation of the profile. Subsequently, a full factorial design was adopted in order to obtain a whole spectrum of barrel shapes. As a result, a total of 225 design cases was generated for the DOE study.

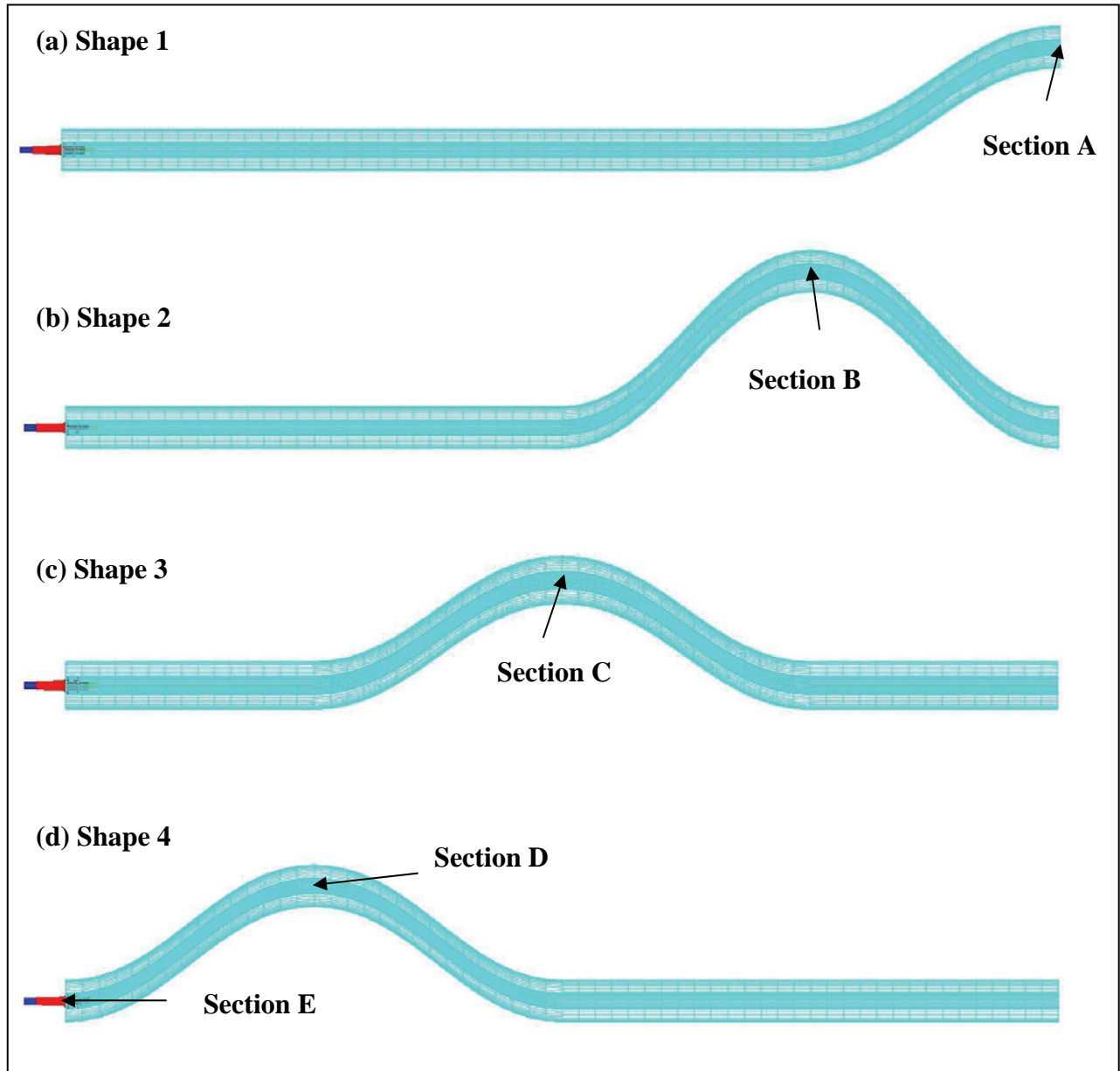


Figure 5. Display of four fundamental deflection shapes of a gun barrel.

Table 1. Absolute lateral displacement (mm) of a gun barrel at five chosen sections.

Level	Section E	Section D	Section C	Section B	Section A
1	0	0.03 (0.0008%)	0.05 (0.0013%)	0.21 (0.0055%)	0.25 (0.0065%)
2		0	0	0.105	0.125
3		-0.03	-0.05	0	0
4				-0.105	-0.125
5				-0.21	-0.25

The details of the 225 design cases are provided in appendix A. Case number 113 that had zero displacement on all section points represents a perfectly straight gun tube. Cases 39 and 189 had a respective maximum value at each point with staggered signs, thus implying highly curved gun tubes. It is worth mentioning that an explicit dynamic analysis of the initial EAPS system was performed with the LS-DYNA¹ tool on the Linux Networx Evolocity II cluster at ARL’s Major Shared Resource Center (see a previous report [1]). The one single analysis required a total of 48 central processing unit (CPU) hours, i.e., 6-hour run with eight processors in parallel. It would therefore be too cumbersome to run through the entire 225 design cases with the original configuration. Because the time step used for the analysis depends on the size of the smallest element in the model, the geometry was simplified as described in the previous section, which avoided very fine mesh in the nose and fin areas and significantly decreased the computational time to 8 CPU hours. As a result, the execution for the entire 225 design cases became feasible. In-bore structural analysis was then performed and the muzzle responses were obtained from each case. The translational velocity responses of the projectile at the exit are given in appendix B. In addition, appendix C provides muzzle yaw angle and yaw rate for each case. The responses of pitch angle and pitch rate are also provided in appendix D. To evaluate the significance of each shape variable, the analysis of variance (ANOVA) method was employed to assess the results.

4. Analysis of Variance

Projectile responses at the muzzle serve as initial conditions for aerodynamics in exterior ballistics and therefore are critical to overall performance. Three translational velocity components, i.e., axial (X), lateral (Y), and vertical (Z) components, of rigid body motion were obtained from each of the design cases. In addition, rotational velocity components, such as yaw rate and pitch rate, are also important and of interest in this study. Since the EAPS is a fin-stabilized projectile and fired with a smooth bore, roll angular velocity is ignored. In addition, because muzzle responses were extracted in rigid body mode, the principal axis of the projectile can be assumed to remain a straight line during in-bore travel. In order to compute yaw and pitch angles, position vectors for the tip of the projectile with respect to the CG at Y and Z directions, representing the heading

¹LS-DYNA, which is not an acronym, is a trademark of Livermore Software Technology Corporation.

direction of the projectile, were computed. Based on the position vectors, the corresponding yaw and pitch angles were then calculated. By the definition of angular rates, the yaw and pitch velocities could be derived when the changes of the angles were obtained at two consecutive small time steps.

The ANOVA method was employed to estimate error variance and to determine the relative importance of various factors, i.e., barrel shapes and their interactions. Figure 6 shows the contributing percentage of the four barrel shape variables and their interactions with X, Y, and Z velocities, respectively. A total of 11 contributing sources, four main effects plus six interactions and one error term, were illustrated in the bar charts. From figure 6(a), the combination of shapes 3 and 4 contributed more than 50% to X velocity. The total contributions from the interaction terms appear to be considerably high. For Y velocity, the majority was affected by the shape 1 variable alone, and the level of importance decreased with the location away from the muzzle. Surprisingly, the cross terms between the shape 1 and the other shape variables appear to have little effect on the response. Figure 6(c) indicates that the shape 4 variable contributes to Z velocity more than the others, but the difference was not substantial.

Similarly, the contributing percentage of the shape variables to the responses of yaw and pitch angles at the muzzle was also obtained and is shown in figure 7. It can be seen that more than 30% of yaw angle variations are explained by the shape 4 variable while the other shapes each contribute less than 20%. From figure 7(b), shapes 1 and 4 appeared to be more highly significant than the other two shapes to the pitch angle variations. The significance of the shape 4 variable could be because the peak acceleration took place at the location where the deflection was simulated. In other words, the projectile passed through the deformed area when it was accelerated the most, which led to higher lateral and vertical accelerations. As a result, it substantially affected the pitch and yaw angles at the muzzle. Figure 8 demonstrates the level of influence of the yaw and pitch rates by the shape variables. Apparently, the deflections near the muzzle area exhibit great impact on both angular velocities. Figure 8(a) indicates that more than 85% of the yaw rate variations were contributed by the shape 1 and 2 variables. Dramatically, the shape 1 variable alone accounted for 62% of pitch rate variations as shown in figure 8(b). The contributing percentages of the interaction terms were all marginal except the one between shape 1 and shape 2 to yaw rate response.

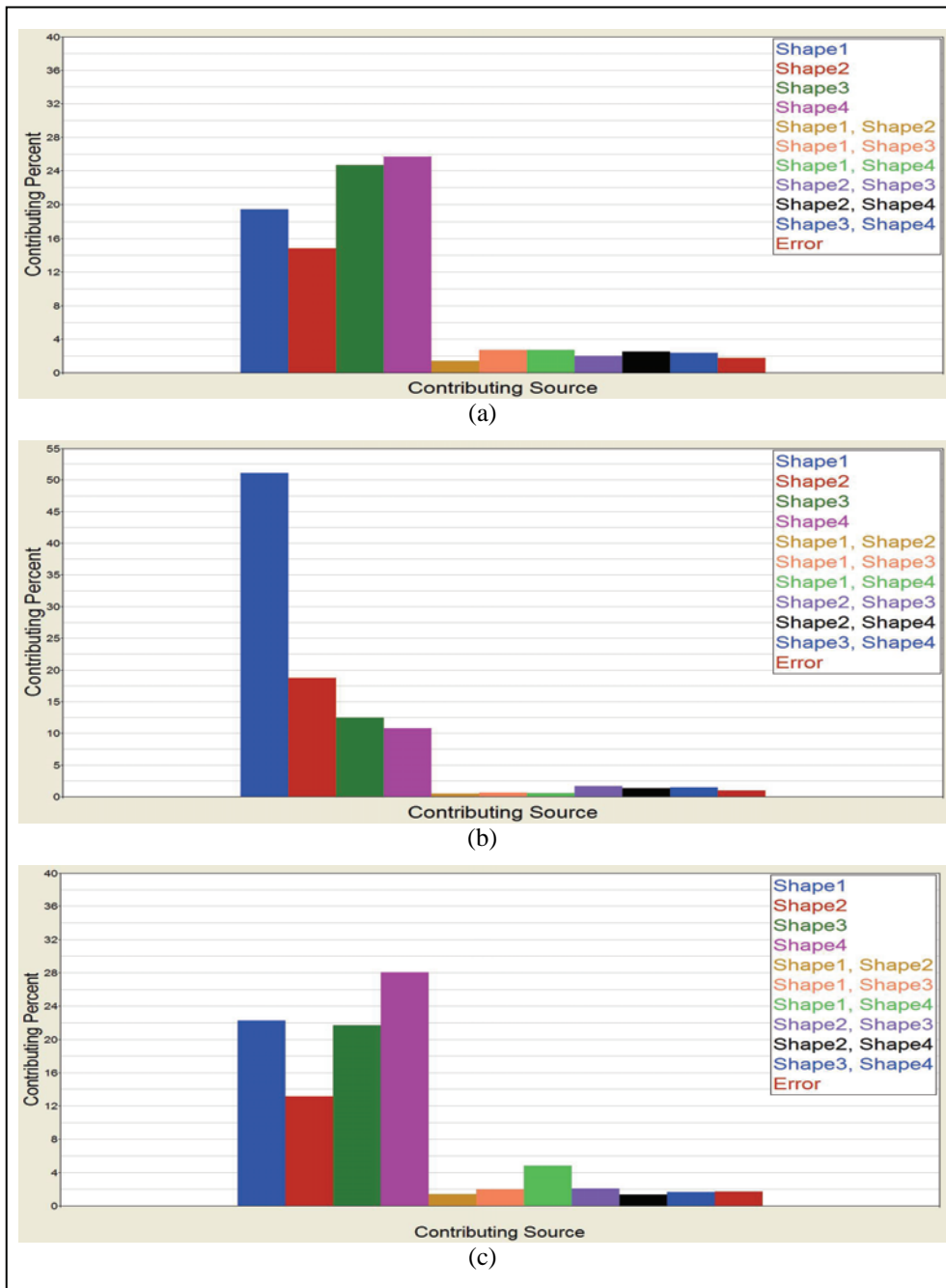


Figure 6. Comparison of contributing percentage of four barrel shapes and their interactions with (a) axial velocity, (b) lateral velocity, and (c) vertical velocity.

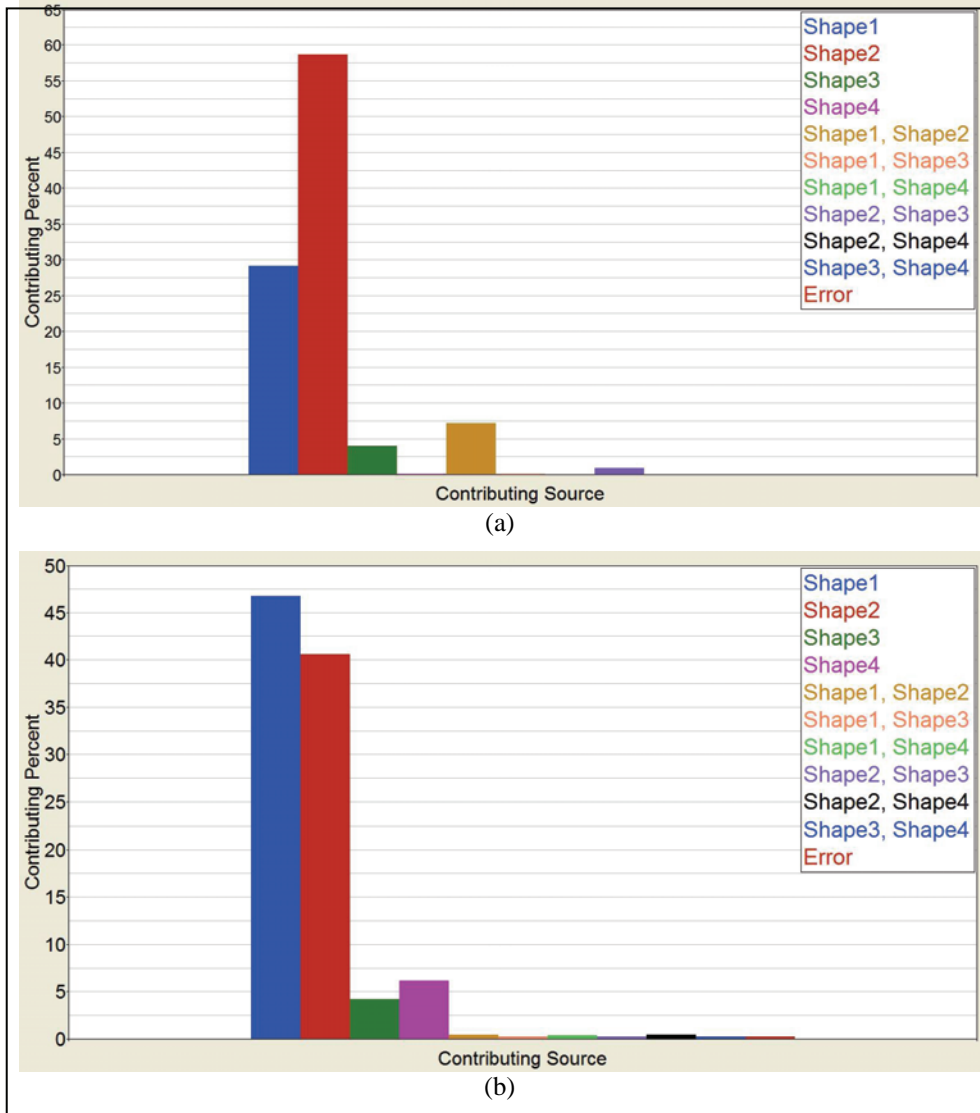


Figure 7. Comparison of contributing percentage of four barrel shapes and their interactions with (a) yaw angle and (b) pitch angle.

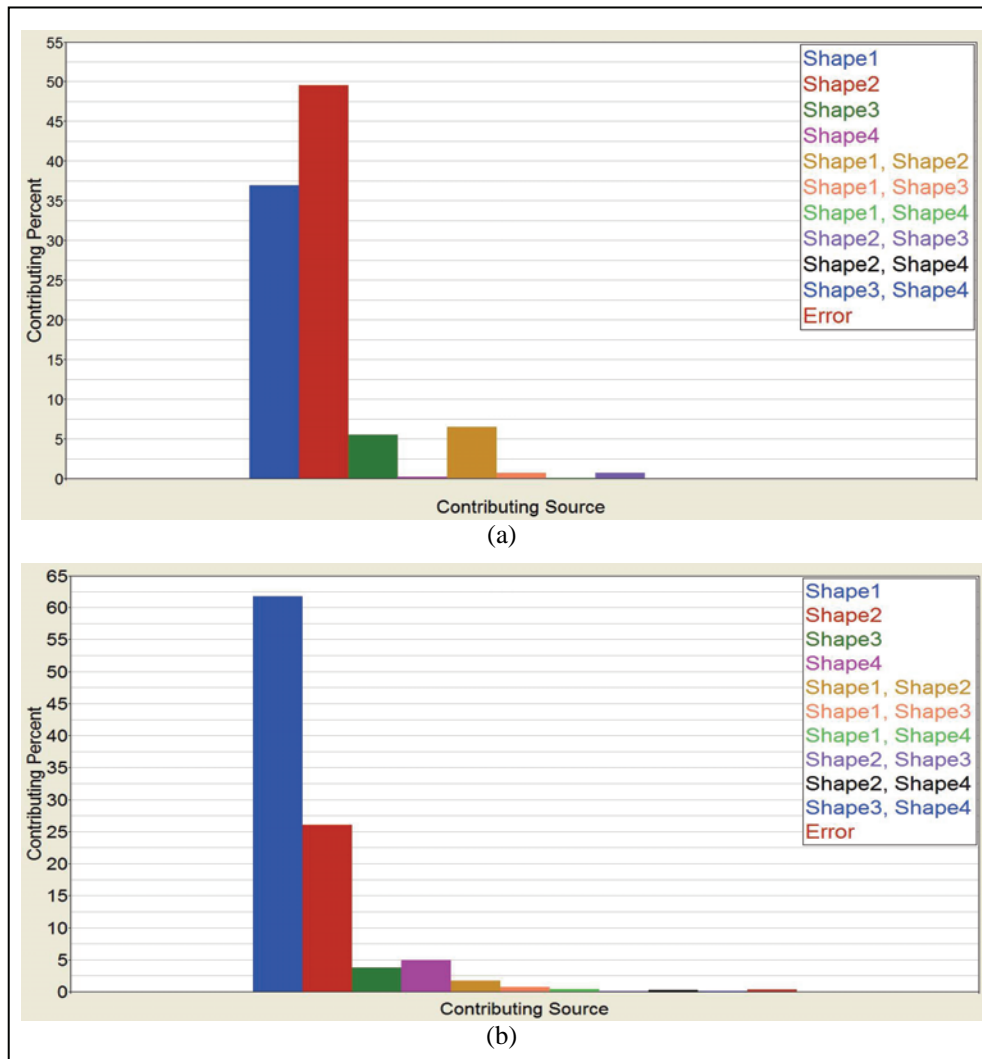


Figure 8. Comparison of contributing percentage of four barrel shapes and their interactions with (a) yaw rate and (b) pitch rate.

A response surface model that fitted the observed 225 data was derived for each of the muzzle velocity components. A complete high order polynomial was adopted, which consists of a total of 64 regression coefficients, fourth order for shapes 1 and 2 because five levels of data are in use, and second order for shapes 3 and 4 because of three levels of data. The residual plots for the X, Y, and Z velocities are shown in figure 9(a), (b), and (c), respectively. It depicts the differences between the observed response values from the exact analysis solver and the predicted response values from the regression model. A displayed straight line in each plot represents the place where the predicted and observed values match each other. Overall, the wide scatter of the residuals indicates that the response surface models failed to provide good predictions on the responses. The R-squared values for the fits of X, Y, and Z velocities were 0.31, 0.64, and 0.30, respectively. The values could be interpreted as the proportion in the data variability explained by the regression model. The results demonstrated that the Y velocity response served a better candidate for prediction.

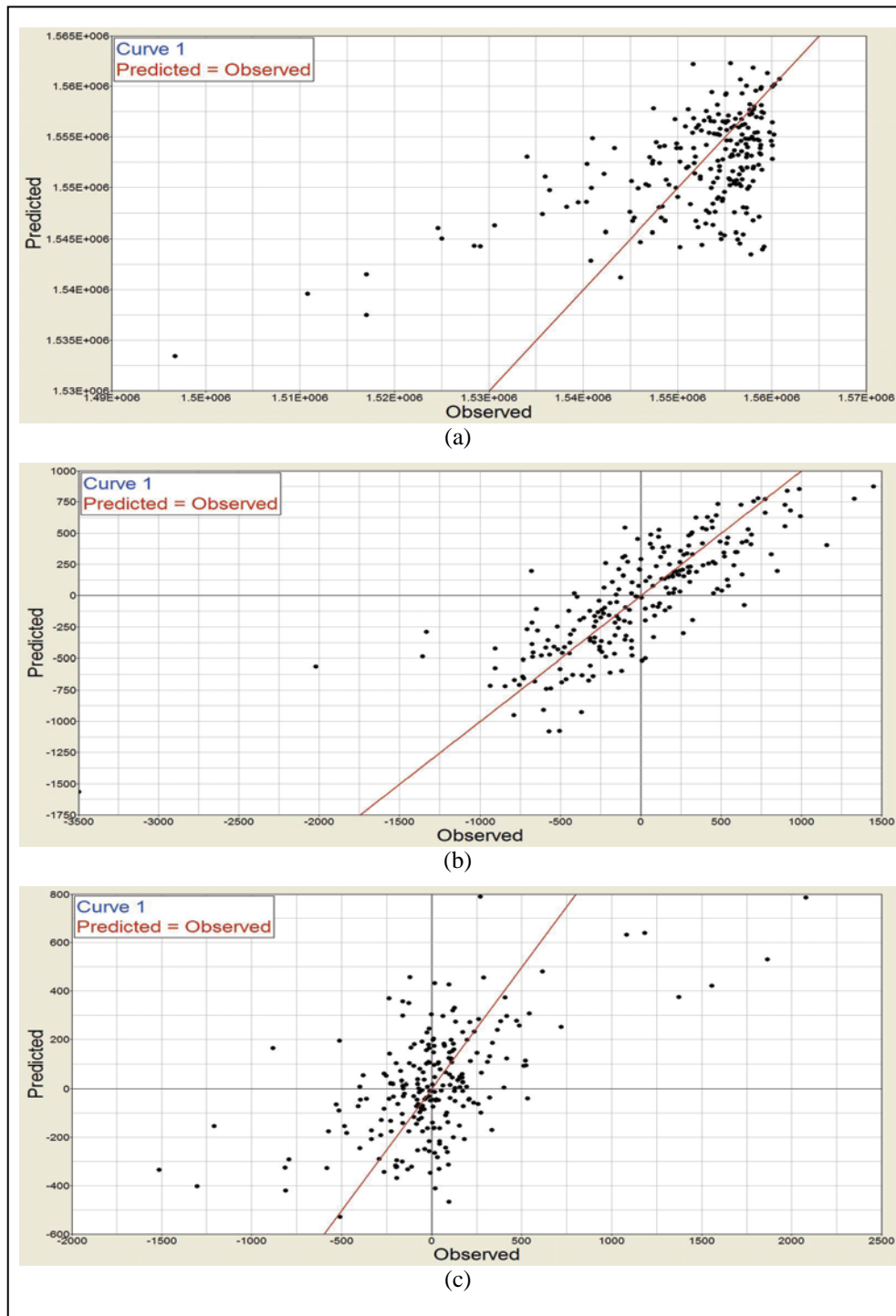


Figure 9. Residual plots of projectile (a) X, (b) Y, and (c) Z velocities at the muzzle.

In addition, complete high-order polynomial response surface models were obtained for angular velocities as well. Figure 10(a) and (b) shows the residuals of predicted yaw and pitch rates, respectively, against observed values. Since the simulated lateral displacements of gun barrels are expected to directly influence the yaw angle of in-bore projectile, not surprisingly, the predicted and observed values had very good agreement as shown in figure 10(a). It indicates that the yaw

rate can be well predicted with the response surface model, as given in appendix E. The pitch rates appear to group closer to the straight line at higher values, as shown in figure 10(b). Overall, the residuals of pitch rates show smaller values in magnitude. The fittings of yaw and pitch rates both exhibited high R-squared values.

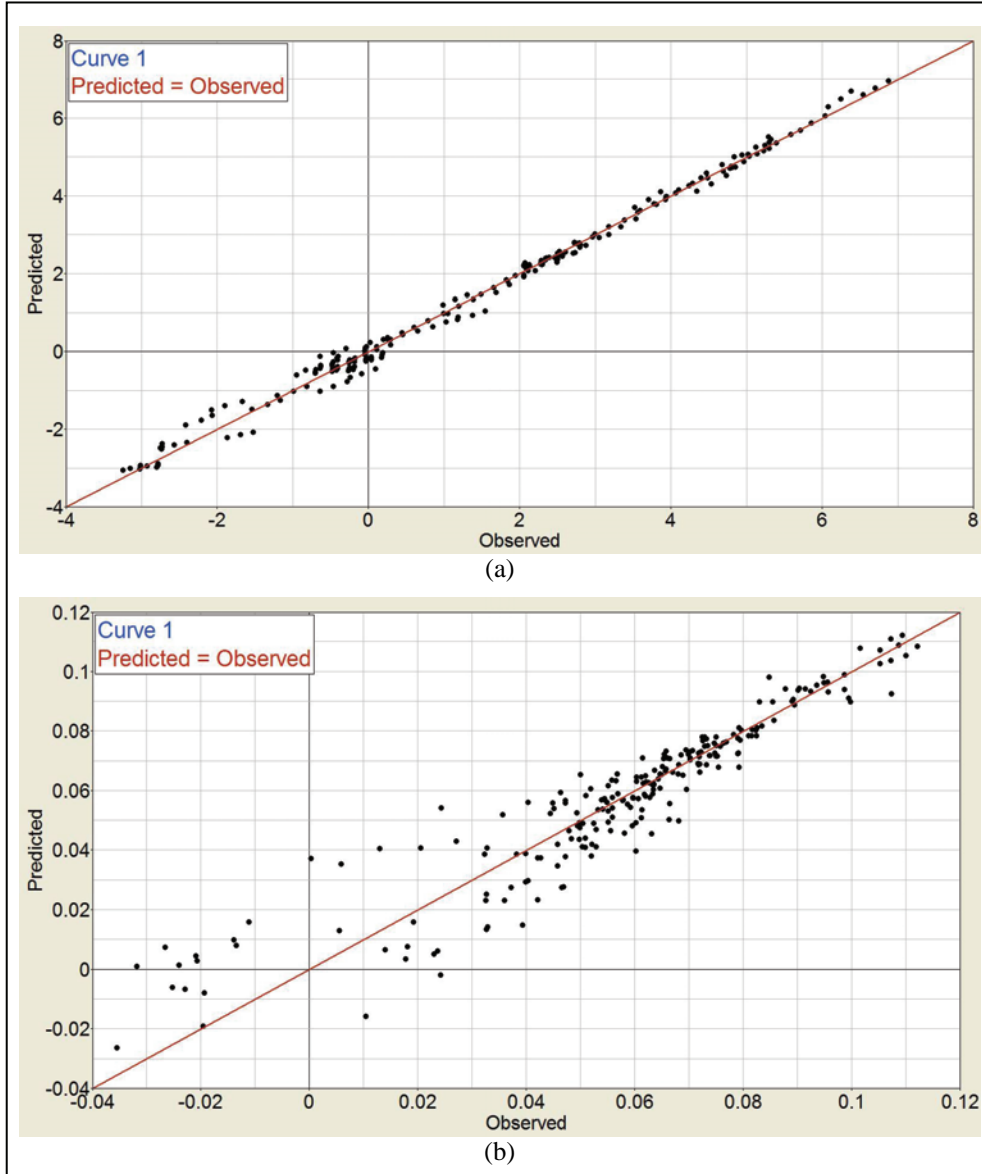


Figure 10. Residual plots of projectile (a) yaw rate and (b) pitch rate at the muzzle.

5. Response Statistics

It is always interesting to study the statistical property of the responses and to assess the sensitivity of the responses to the shape variables after in-bore structural analyses have been solved against a total of 225 distinct barrel shapes. Response statistics, including mean value, standard deviation, maximum and minimum values for the translational X, Y, and Z velocities, are summarized in table 2. Understandably, the contribution of gun barrel flexure to the deviations of X velocity was negligible because of a small coefficient of variation (0.5%) for the response. In addition, the range of the maximum and minimum X velocity was considerably narrow, implying marginal effect of the deformed gun tubes. As expected, the mean values of the other responses were virtually zero because of symmetric gun shapes (i.e., bent on both positive and negative sides) being used. Notice that the response distribution of the Y velocity was somewhat left skewed. It may be because the response was highly sensitive to the modeling tolerance including the gun barrels and the projectile system. In addition, it can be seen that the standard deviations of the responses were all substantially high, which further warrants strong sensitivity of the responses to the barrel centerline variations.

Table 2. Response statistics of projectile translational velocity at the muzzle from DOE analysis.

	X-Velocity (mm/sec)	Y-Velocity (mm/sec)	Z-Velocity (mm/sec)
Average	1.5523 x10 ⁶	-18.9	13.2
Standard Deviation	8.657 x10 ³	542.6	388
Maximum	1.5608 x10 ⁶	1449	2078
Minimum	1.4968 x10 ⁶	-3497	-1513

Table 3 provides the response statistics of rotational angles as well as of rotational rates at the muzzle. The yaw responses exhibited very high coefficient of variations, suggesting the responses be significantly influenced by the gun barrel shapes. Because of the symmetry of the design set, the magnitudes of the maximum and minimum values for both yaw angle and yaw rate yielded quite closely as expected. The change of the sign simply represents the opposite direction. On the other hand, the pitch angle and pitch rate responses appear not to be as normally distributed as the yaw responses. In addition, the level of variations was relatively low, explaining that the pitch responses were less impacted by the gun shapes.

Table 3. Response statistics of projectile rotational angle and rotational rate at the muzzle from DOE analysis.

	Yaw Angle (degree)	Yaw Rate (degree/sec)	Pitch Angle (degree)	Pitch Rate (degree/sec)
Average	3.60E-05	-3.28E-02	-1.07E-05	-6.37E-02
Standard Deviation	4.10E-04	5.295	5.94E-06	1.90E-02
Maximum	8.55E-04	1.07E+01	6.35E-07	-2.37E-02
Minimum	-7.80E-04	-1.08E+01	-2.58E-05	-1.12E-01

To further understand how the responses reacted to a change in the levels of the shape variables, the main effect (*IO*) of each controlled factor alone was computed. The changes in X, Y, and Z velocities by a shift in the levels of the four shape variables are shown in figure 11. The controlled design variables referred to the number of levels chosen for each barrel shape in DOE. The two end points of each linear segment represent the change from one level to another. Apparently, the levels of the shape 1 variable demonstrated significant influences on the Y velocity as opposed to the other two responses. The changes of the Y velocity response appear to be linearly proportional to the changes of the levels of the factor. The X velocity is shown to reach a highest value of 1555 m/sec when the gun bore came with no deflection at the muzzle. It is also expected that the Y velocity was close to neutral with a gun barrel having a perfectly straight centerline, as demonstrated in figure 11(b). The main effects of the barrel shapes seemed to differ marginally on the Z velocity and exhibited no obvious pattern.

6. Summary

The effects of deformed gun tubes on the EAPS projectile launch dynamics were studied. An in-bore dynamic analysis was performed for the launch of a 60-mm projectile system with a gun barrel that has characteristic centerline variations in recent study. The results demonstrated significant response deviations as opposed to those computed for the system simulated with a perfectly straight gun tube. In order to assess the overall effects, a parametric model, which included four shape variables representing displacement at lateral direction, for the gun barrel was developed. The values of each shape variable were assigned a certain number of levels that were determined by the measurement data from an array of experimental gun barrels. The DOE methodology was employed for the parametric study. A total of 225 cases was created, based on a full factorial design. Each case yielded a dissimilar barrel shape so that the entire design set formed a good representation of the barrel centerline variations profile. Explicit dynamic analysis was then performed on each case throughout the whole design set, and the results for the projectile responses at the muzzle were obtained. For computational efficiency, the geometry of the EAPS projectile was slightly altered without a change in the CG.

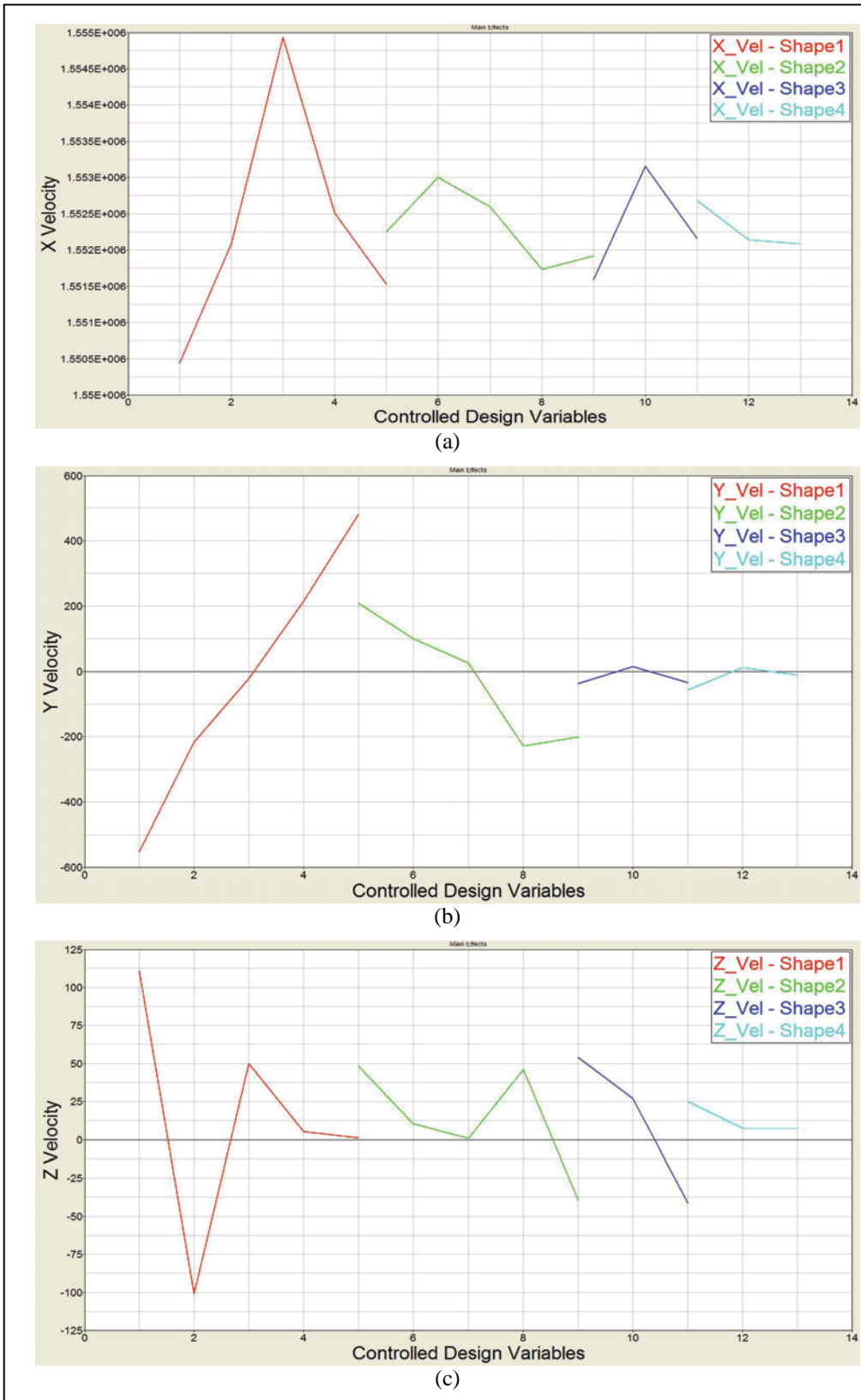


Figure 11. Changes in (a) X, (b) Y, and (c) Z velocities by a change in the levels of the four barrel shapes.

Responses of the projectile at the muzzle, such as translational and rotational velocities, were computed. The ANOVA technique was adopted to evaluate the significance of the shape variables. It was found that the exit lateral velocity was highly sensitive to the deflection mode at the muzzle while the other shape variables showed little contribution. The axial velocity was marginally affected by the barrel centerline variations. No outstanding distinction was exhibited among the shape variables. The influence of the lateral displacement closer to chamber region was slightly greater on vertical velocity than the influence of the other regions. The flexure near the muzzle area demonstrated a significant contribution to angular velocity including yaw and pitch rates. A response surface model that consisted of a complete high-order polynomial based on the four shape variables was derived for each individual response datum. Residual plots were generated to describe the goodness of fits and the yaw rate were found to be the best candidate for prediction. Finally, responses statistics were calculated to assess the range and distribution of the muzzle responses. The symmetry of the results, such as Y and Z velocity, conformed to the property of the DOE design, and the high coefficient of variations further warranted strong response sensitivity to the centerline deviations. Finally, the transverse-to-axial velocity ratio can be calculated from the response statistics. Neglecting the covariance between the transverse and axial velocities, the standard deviation of the ratio is estimated to be 0.35 mrad. Furthermore, the aerodynamic jump of 0.59 mrad and the maximum angle of attack of 0.15 degree are computed on the basis of 97% likelihood of occurrence. The 225 simulated gun shapes used in this study are in accordance with reasonable gun tube manufacturing tolerance. This implies that no erratic launch of the EAPS projectile is anticipated because of the barrel centerline variations.

7. References

1. Chen M. *Structural Design and Analysis of Initial Extended Area Protection and Survivability (EAPS) Projectile Configurations*; ARL-TR-3866; U.S. Army Research Laboratory: Aberdeen Proving Ground, MD, August 2006.
2. Chen M. Structural Design and Analysis of Hit-to-Kill Projectile. *9th International LS-DYNA Users Conference*, Dearborn, Michigan, USA, Session 2, 13-22, 2006.
3. Watson, C.; Knapton, J. D.; Boyer, N.; Stobie, C. *Sensitivity of Muzzle Velocity Repeatability to Variations in Initial Conditions*; BRL-TR-3323; Ballistic Research Laboratory: Aberdeen Proving Ground, MD, March 1992.
4. Thomas, J.; Wren, G.; Coffee, T.; Richardson, S. *Muzzle Velocity Sensitivity Based on Interior Ballistic Modeling*; ARL-MR-110; U.S. Army Research Laboratory: Aberdeen Proving Ground, MD, September 1993.
5. Oberle, W.; Wren G. *Estimating Muzzle Velocity Variability in a Regenerative Liquid Propellant Gun through Stochastic Modeling*; ARL-TR-746; U.S. Army Research Laboratory: Aberdeen Proving Ground, MD, June 1995.
6. Erline, T. *Deviation Effect of an In-Bore Centerline on a 5-Inch Naval Gun*; ARL-MR-492; U.S. Army Research Laboratory: Aberdeen Proving Ground, MD, September 2000.
7. Bundy, M.; Newill, J. *A Methodology for Characterizing Barrel Flexure Due to Tank Motion*; ARL-MR-479; U.S. Army Research Laboratory: Aberdeen Proving Ground, MD, June 2000.
8. Bundy, M.; Newill, J.; Marcopoli, V.; Ng, M.; Wells, C. A Methodology for Characterizing Gun Barrel Flexure Due to Vehicle Motion. *Shock and Vibration* **2001**, 8, 223-228.
9. Newill, J.; Garner, J.; Bundy, M. *Methodology for Determining Optimal Tank Cannon Barrel Centerline Shape*; ARL-TR-2813; U.S. Army Research Laboratory: Aberdeen Proving Ground, MD, September 2002.
10. Altair Engineering, Inc. Help Manual of HyperStudy 7.0, Troy, MI, 2005.

INTENTIONALLY LEFT BLANK

Appendix A. List of Lateral Displacement (millimeters) for the Level Combination of Four Barrel Shape Variables in DOE Design

Run #	Shape1	Shape2	Shape3	Shape4	Run #	Shape1	Shape2	Shape3	Shape4
1	-0.25	-0.21	-0.05	-0.03	114	0	0	0	0.03
2	-0.25	-0.21	-0.05	0	115	0	0	0.05	-0.03
3	-0.25	-0.21	-0.05	0.03	116	0	0	0.05	0
4	-0.25	-0.21	0	-0.03	117	0	0	0.05	0.03
5	-0.25	-0.21	0	0	118	0	0.105	-0.05	-0.03
6	-0.25	-0.21	0	0.03	119	0	0.105	-0.05	0
7	-0.25	-0.21	0.05	-0.03	120	0	0.105	-0.05	0.03
8	-0.25	-0.21	0.05	0	121	0	0.105	0	-0.03
9	-0.25	-0.21	0.05	0.03	122	0	0.105	0	0
10	-0.25	-0.105	-0.05	-0.03	123	0	0.105	0	0.03
11	-0.25	-0.105	-0.05	0	124	0	0.105	0.05	-0.03
12	-0.25	-0.105	-0.05	0.03	125	0	0.105	0.05	0
13	-0.25	-0.105	0	-0.03	126	0	0.105	0.05	0.03
14	-0.25	-0.105	0	0	127	0	0.21	-0.05	-0.03
15	-0.25	-0.105	0	0.03	128	0	0.21	-0.05	0
16	-0.25	-0.105	0.05	-0.03	129	0	0.21	-0.05	0.03
17	-0.25	-0.105	0.05	0	130	0	0.21	0	-0.03
18	-0.25	-0.105	0.05	0.03	131	0	0.21	0	0
19	-0.25	0	-0.05	-0.03	132	0	0.21	0	0.03
20	-0.25	0	-0.05	0	133	0	0.21	0.05	-0.03
21	-0.25	0	-0.05	0.03	134	0	0.21	0.05	0
22	-0.25	0	0	-0.03	135	0	0.21	0.05	0.03
23	-0.25	0	0	0	136	0.125	-0.21	-0.05	-0.03
24	-0.25	0	0	0.03	137	0.125	-0.21	-0.05	0
25	-0.25	0	0.05	-0.03	138	0.125	-0.21	-0.05	0.03
26	-0.25	0	0.05	0	139	0.125	-0.21	0	-0.03
27	-0.25	0	0.05	0.03	140	0.125	-0.21	0	0
28	-0.25	0.105	-0.05	-0.03	141	0.125	-0.21	0	0.03
29	-0.25	0.105	-0.05	0	142	0.125	-0.21	0.05	-0.03
30	-0.25	0.105	-0.05	0.03	143	0.125	-0.21	0.05	0
31	-0.25	0.105	0	-0.03	144	0.125	-0.21	0.05	0.03
32	-0.25	0.105	0	0	145	0.125	-0.105	-0.05	-0.03
33	-0.25	0.105	0	0.03	146	0.125	-0.105	-0.05	0
34	-0.25	0.105	0.05	-0.03	147	0.125	-0.105	-0.05	0.03
35	-0.25	0.105	0.05	0	148	0.125	-0.105	0	-0.03
36	-0.25	0.105	0.05	0.03	149	0.125	-0.105	0	0
37	-0.25	0.21	-0.05	-0.03	150	0.125	-0.105	0	0.03
38	-0.25	0.21	-0.05	0	151	0.125	-0.105	0.05	-0.03
39	-0.25	0.21	-0.05	0.03	152	0.125	-0.105	0.05	0
40	-0.25	0.21	0	-0.03	153	0.125	-0.105	0.05	0.03
41	-0.25	0.21	0	0	154	0.125	0	-0.05	-0.03
42	-0.25	0.21	0	0.03	155	0.125	0	-0.05	0
43	-0.25	0.21	0.05	-0.03	156	0.125	0	-0.05	0.03
44	-0.25	0.21	0.05	0	157	0.125	0	0	-0.03
45	-0.25	0.21	0.05	0.03	158	0.125	0	0	0
46	-0.125	-0.21	-0.05	-0.03	159	0.125	0	0	0.03
47	-0.125	-0.21	-0.05	0	160	0.125	0	0.05	-0.03
48	-0.125	-0.21	-0.05	0.03	161	0.125	0	0.05	0
49	-0.125	-0.21	0	-0.03	162	0.125	0	0.05	0.03
50	-0.125	-0.21	0	0	163	0.125	0.105	-0.05	-0.03
51	-0.125	-0.21	0	0.03	164	0.125	0.105	-0.05	0
52	-0.125	-0.21	0.05	-0.03	165	0.125	0.105	-0.05	0.03
53	-0.125	-0.21	0.05	0	166	0.125	0.105	0	-0.03

54	-0.125	-0.21	0.05	0.03	167	0.125	0.105	0	0
55	-0.125	-0.105	-0.05	-0.03	168	0.125	0.105	0	0.03
56	-0.125	-0.105	-0.05	0	169	0.125	0.105	0.05	-0.03
57	-0.125	-0.105	-0.05	0.03	170	0.125	0.105	0.05	0
58	-0.125	-0.105	0	-0.03	171	0.125	0.105	0.05	0.03
59	-0.125	-0.105	0	0	172	0.125	0.21	-0.05	-0.03
60	-0.125	-0.105	0	0.03	173	0.125	0.21	-0.05	0
61	-0.125	-0.105	0.05	-0.03	174	0.125	0.21	-0.05	0.03
62	-0.125	-0.105	0.05	0	175	0.125	0.21	0	-0.03
63	-0.125	-0.105	0.05	0.03	176	0.125	0.21	0	0
64	-0.125	0	-0.05	-0.03	177	0.125	0.21	0	0.03
65	-0.125	0	-0.05	0	178	0.125	0.21	0.05	-0.03
66	-0.125	0	-0.05	0.03	179	0.125	0.21	0.05	0
67	-0.125	0	0	-0.03	180	0.125	0.21	0.05	0.03
68	-0.125	0	0	0	181	0.25	-0.21	-0.05	-0.03
69	-0.125	0	0	0.03	182	0.25	-0.21	-0.05	0
70	-0.125	0	0.05	-0.03	183	0.25	-0.21	-0.05	0.03
71	-0.125	0	0.05	0	184	0.25	-0.21	0	-0.03
72	-0.125	0	0.05	0.03	185	0.25	-0.21	0	0
73	-0.125	0.105	-0.05	-0.03	186	0.25	-0.21	0	0.03
74	-0.125	0.105	-0.05	0	187	0.25	-0.21	0.05	-0.03
75	-0.125	0.105	-0.05	0.03	188	0.25	-0.21	0.05	0
76	-0.125	0.105	0	-0.03	189	0.25	-0.21	0.05	0.03
77	-0.125	0.105	0	0	190	0.25	-0.105	-0.05	-0.03
78	-0.125	0.105	0	0.03	191	0.25	-0.105	-0.05	0
79	-0.125	0.105	0.05	-0.03	192	0.25	-0.105	-0.05	0.03
80	-0.125	0.105	0.05	0	193	0.25	-0.105	0	-0.03
81	-0.125	0.105	0.05	0.03	194	0.25	-0.105	0	0
82	-0.125	0.21	-0.05	-0.03	195	0.25	-0.105	0	0.03
83	-0.125	0.21	-0.05	0	196	0.25	-0.105	0.05	-0.03
84	-0.125	0.21	-0.05	0.03	197	0.25	-0.105	0.05	0
85	-0.125	0.21	0	-0.03	198	0.25	-0.105	0.05	0.03
86	-0.125	0.21	0	0	199	0.25	0	-0.05	-0.03
87	-0.125	0.21	0	0.03	200	0.25	0	-0.05	0
88	-0.125	0.21	0.05	-0.03	201	0.25	0	-0.05	0.03
89	-0.125	0.21	0.05	0	202	0.25	0	0	-0.03
90	-0.125	0.21	0.05	0.03	203	0.25	0	0	0
91	0	-0.21	-0.05	-0.03	204	0.25	0	0	0.03
92	0	-0.21	-0.05	0	205	0.25	0	0.05	-0.03
93	0	-0.21	-0.05	0.03	206	0.25	0	0.05	0
94	0	-0.21	0	-0.03	207	0.25	0	0.05	0.03
95	0	-0.21	0	0	208	0.25	0.105	-0.05	-0.03
96	0	-0.21	0	0.03	209	0.25	0.105	-0.05	0
97	0	-0.21	0.05	-0.03	210	0.25	0.105	-0.05	0.03
98	0	-0.21	0.05	0	211	0.25	0.105	0	-0.03
99	0	-0.21	0.05	0.03	212	0.25	0.105	0	0
100	0	-0.105	-0.05	-0.03	213	0.25	0.105	0	0.03
101	0	-0.105	-0.05	0	214	0.25	0.105	0.05	-0.03
102	0	-0.105	-0.05	0.03	215	0.25	0.105	0.05	0
103	0	-0.105	0	-0.03	216	0.25	0.105	0.05	0.03
104	0	-0.105	0	0	217	0.25	0.21	-0.05	-0.03
105	0	-0.105	0	0.03	218	0.25	0.21	-0.05	0
106	0	-0.105	0.05	-0.03	219	0.25	0.21	-0.05	0.03
107	0	-0.105	0.05	0	220	0.25	0.21	0	-0.03
108	0	-0.105	0.05	0.03	221	0.25	0.21	0	0
109	0	0	-0.05	-0.03	222	0.25	0.21	0	0.03
110	0	0	-0.05	0	223	0.25	0.21	0.05	-0.03
111	0	0	-0.05	0.03	224	0.25	0.21	0.05	0
112	0	0	0	-0.03	225	0.25	0.21	0.05	0.03
113	0	0	0	0					

Appendix B. Response Values of Translational Velocity (millimeters per second) at the Muzzle From DOE Analysis

Run #	X Velocity	Y Velocity	Z Velocity	Run #	X Velocity	Y Velocity	Z Velocity
1	1535707	-1333.4	2077.9	114	1559736	-148.2	-28.7
2	1559171	-54.7	72.5	115	1528453	-2022.3	322.5
3	1550270	-256.8	-162.1	116	1555179	323.8	10.6
4	1554782	-286.4	268.8	117	1557262	-139.3	-78.1
5	1558757	88.0	133.3	118	1554973	-315.6	117.6
6	1545101	-159.0	1183.1	119	1553720	-366.7	-0.6
7	1556740	-69.7	-237.3	120	1552527	-518.6	90.5
8	1554817	29.8	-100.7	121	1547419	75.0	-75.5
9	1535988	-18.6	109.7	122	1556746	-135.6	-143.1
10	1556212	7.4	-120.5	123	1558802	-395.3	77.2
11	1556607	-658.1	2.8	124	1536417	-91.3	415.7
12	1557363	-191.0	320.4	125	1560006	-57.1	235.4
13	1540406	-1358.7	1556.3	126	1558877	-414.3	-335.1
14	1555549	-443.7	102.0	127	1557502	-354.1	-1.8
15	1555071	-119.9	406.6	128	1557877	-197.7	-172.6
16	1538218	-732.4	-1210.1	129	1553065	-30.7	-193.7
17	1540872	-618.7	-510.0	130	1558483	-439.6	-265.8
18	1558725	-577.8	-201.0	131	1551628	-150.5	523.2
19	1548102	-243.0	614.7	132	1556846	-68.3	-22.1
20	1554442	-567.2	252.3	133	1556921	-314.4	-48.2
21	1547463	-674.6	542.8	134	1557663	-285.8	212.3
22	1558922	-290.7	-15.2	135	1555843	-267.2	-278.9
23	1556852	-279.4	157.7	136	1555193	145.6	62.4
24	1554201	-904.6	-127.9	137	1534071	1157.8	-573.4
25	1557424	-297.7	17.6	138	1556960	520.9	15.6
26	1556143	-164.6	42.7	139	1547358	579.3	107.7
27	1557863	-515.4	-41.0	140	1557903	313.5	-166.5
28	1543974	-506.2	1081.0	141	1529074	-678.9	1373.8
29	1496763	-3496.7	-880.8	142	1556544	450.0	-363.9
30	1556346	-570.9	309.6	143	1560065	113.7	-163.9
31	1550010	-424.7	415.2	144	1557761	688.2	12.2
32	1547341	-368.7	-84.0	145	1558304	299.1	144.8
33	1550321	-735.6	-253.6	146	1554066	299.1	-81.2
34	1557966	-466.0	213.4	147	1553852	58.8	-16.7
35	1551944	-787.9	42.5	148	1551714	850.6	-123.5
36	1560010	-591.9	-38.5	149	1549885	110.5	101.1
37	1553969	-559.6	-18.3	150	1550969	244.0	289.1
38	1542389	-605.2	-283.3	151	1553756	266.5	-13.4
39	1548061	-726.6	-400.1	152	1553504	659.6	335.0
40	1557846	-588.8	112.7	153	1553034	384.5	-227.4
41	1553314	-844.2	-56.1	154	1560026	229.6	45.1
42	1555594	-787.1	-400.6	155	1560813	173.1	-73.3
43	1530632	-938.1	-51.8	156	1555135	387.2	-159.5
44	1557384	-491.9	91.8	157	1555846	-55.6	-7.2
45	1554308	-676.4	40.2	158	1552820	494.6	13.1
46	1558056	174.7	-379.5	159	1558068	77.8	124.7
47	1556018	208.4	-196.5	160	1539450	-708.5	-793.9
48	1554717	29.0	23.6	161	1558345	198.6	-65.4
49	1558896	3.5	3.9	162	1555528	475.6	-30.9
50	1548120	-9.3	-811.7	163	1555353	-189.8	-115.2
51	1554222	-291.1	-78.0	164	1555429	264.0	96.5
52	1554263	-318.6	175.3	165	1557719	-134.3	115.0

53	1551986	-177.1	-113.4	166	1559085	-109.6	-189.7
54	1540324	107.1	126.0	167	1558175	305.7	52.8
55	1556593	-260.2	170.0	168	1556849	462.0	-100.0
56	1544959	452.7	181.8	169	1555114	-54.9	-24.3
57	1547768	-675.7	99.7	170	1553878	-226.9	512.5
58	1555621	-248.3	-127.5	171	1543296	541.2	155.6
59	1556043	-12.3	-265.4	172	1551887	31.5	154.2
60	1556541	-56.2	-197.2	173	1554245	346.2	-66.8
61	1557286	-99.6	87.7	174	1557315	-113.3	-51.2
62	1524629	-94.3	-1304.7	175	1554216	150.7	-408.7
63	1553355	-417.1	84.5	176	1558096	56.3	-65.1
64	1557665	-153.0	36.2	177	1552959	158.1	68.4
65	1557281	-6.2	192.9	178	1540791	-241.2	533.5
66	1554352	-649.3	488.2	179	1557582	-109.2	-234.4
67	1548784	644.5	-814.6	180	1510818	813.4	36.0
68	1549110	-97.5	-583.3	181	1558820	731.2	8.7
69	1551820	-101.4	-11.5	182	1554590	775.3	258.3
70	1548371	29.3	102.6	183	1517033	-98.6	-1513.0
71	1552412	-226.4	172.8	184	1552210	1330.0	-484.4
72	1549831	-246.2	471.4	185	1554420	987.2	168.5
73	1555992	-538.7	6.7	186	1554555	409.6	204.3
74	1552599	-324.4	-157.2	187	1559492	701.5	31.2
75	1557433	-217.2	-73.4	188	1556637	910.1	234.3
76	1551113	-446.7	-133.1	189	1558003	773.2	-293.1
77	1546641	-379.4	95.2	190	1558085	622.7	-215.9
78	1556761	-158.9	-78.9	191	1548241	993.6	-25.1
79	1559932	-436.8	-13.5	192	1551774	384.8	129.4
80	1557972	-194.9	-227.6	193	1558934	342.9	-11.1
81	1541001	-233.1	-530.3	194	1556230	897.8	63.3
82	1549755	-473.9	-238.3	195	1547027	630.6	197.7
83	1552405	-312.5	-225.5	196	1555104	667.8	-195.0
84	1542200	-255.2	-160.7	197	1557467	470.4	155.3
85	1550851	-906.1	15.3	198	1556498	442.1	119.2
86	1549879	78.7	-163.3	199	1545835	933.0	-473.0
87	1556878	-503.6	-43.1	200	1559007	479.5	-511.7
88	1551377	-755.4	-159.1	201	1545255	897.6	274.3
89	1556727	-489.8	-54.8	202	1548650	415.7	18.0
90	1554960	-671.3	76.8	203	1525027	1448.9	277.1
91	1548590	421.7	382.1	204	1546060	61.3	-7.8
92	1551585	-217.3	519.3	205	1556827	0.5	-193.2
93	1556441	260.7	-56.6	206	1550245	447.0	-97.3
94	1558653	207.5	170.7	207	1553583	536.2	8.0
95	1560288	73.5	-15.5	208	1555968	131.5	261.2
96	1557206	539.8	11.0	209	1517036	-641.9	1865.9
97	1555793	244.0	120.1	210	1556215	504.2	3.4
98	1555590	96.5	99.8	211	1554486	-20.7	-38.8
99	1558479	310.7	-70.3	212	1558660	296.9	-161.0
100	1553494	322.4	365.5	213	1551139	590.1	-212.4
101	1554424	246.8	336.6	214	1553605	598.5	-263.9
102	1558016	266.3	-151.4	215	1558796	148.7	15.8
103	1555990	196.0	-28.6	216	1553310	318.1	25.0
104	1555310	138.9	107.1	217	1553062	518.2	-516.1
105	1557301	172.1	14.0	218	1545436	180.1	719.0
106	1554783	116.1	38.1	219	1552150	289.7	-15.6
107	1560195	237.7	172.1	220	1557627	-135.5	78.7
108	1555056	299.2	-85.4	221	1556296	122.6	124.9
109	1558564	203.7	47.6	222	1546945	301.5	129.1
110	1555727	219.4	-54.8	223	1557145	631.0	210.3
111	1558872	544.6	-100.3	224	1551692	-82.4	95.1
112	1548653	179.8	-333.7	225	1553811	684.8	-395.9
113	1556737	243.7	400.8				

Appendix C. Response Values of Yaw Angle (degrees) and Yaw Rate (degrees per second) at the Muzzle From DOE Analysis

Run #	Yaw Angle	Yaw Rate	Run #	Yaw Angle	Yaw Rate
1	2.50E-04	-6.92E-01	114	4.21E-05	-4.66E-02
2	2.59E-04	-6.98E-01	115	8.28E-05	1.90E-01
3	2.68E-04	-7.03E-01	116	9.04E-05	1.85E-01
4	3.04E-04	-4.74E-01	117	9.82E-05	1.77E-01
5	3.16E-04	-4.70E-01	118	-2.96E-04	-2.79E+00
6	3.25E-04	-4.81E-01	119	-2.88E-04	-2.80E+00
7	3.63E-04	-2.48E-01	120	-2.77E-04	-2.80E+00
8	3.73E-04	-2.52E-01	121	-2.39E-04	-2.58E+00
9	3.81E-04	-2.60E-01	122	-2.31E-04	-2.57E+00
10	-1.52E-05	-3.23E+00	123	-2.20E-04	-2.58E+00
11	-4.44E-06	-3.23E+00	124	-1.83E-04	-2.35E+00
12	3.35E-06	-3.24E+00	125	-1.75E-04	-2.35E+00
13	4.14E-05	-3.01E+00	126	-1.67E-04	-2.35E+00
14	5.08E-05	-3.01E+00	127	-5.52E-04	-5.29E+00
15	5.73E-05	-3.02E+00	128	-5.43E-04	-5.30E+00
16	9.82E-05	-2.78E+00	129	-5.34E-04	-5.30E+00
17	1.06E-04	-2.78E+00	130	-4.96E-04	-5.07E+00
18	1.15E-04	-2.80E+00	131	-4.89E-04	-5.08E+00
19	-2.74E-04	-5.76E+00	132	-4.78E-04	-5.09E+00
20	-2.65E-04	-5.77E+00	133	-4.40E-04	-4.86E+00
21	-2.57E-04	-5.78E+00	134	-4.34E-04	-4.87E+00
22	-2.19E-04	-5.55E+00	135	-4.23E-04	-4.87E+00
23	-2.11E-04	-5.55E+00	136	6.16E-04	7.54E+00
24	-2.01E-04	-5.55E+00	137	6.25E-04	7.54E+00
25	-1.63E-04	-5.33E+00	138	6.34E-04	7.54E+00
26	-1.56E-04	-5.33E+00	139	6.74E-04	7.76E+00
27	-1.46E-04	-5.33E+00	140	6.81E-04	7.76E+00
28	-5.28E-04	-8.27E+00	141	6.89E-04	7.75E+00
29	-5.19E-04	-8.29E+00	142	7.27E-04	7.99E+00
30	-5.11E-04	-8.27E+00	143	7.34E-04	7.99E+00
31	-4.71E-04	-8.04E+00	144	7.43E-04	7.98E+00
32	-4.62E-04	-8.05E+00	145	3.58E-04	5.04E+00
33	-4.56E-04	-8.07E+00	146	3.67E-04	5.03E+00
34	-4.15E-04	-7.84E+00	147	3.74E-04	5.03E+00
35	-4.07E-04	-7.84E+00	148	4.13E-04	5.26E+00
36	-3.98E-04	-7.84E+00	149	4.22E-04	5.26E+00
37	-7.80E-04	-1.08E+01	150	4.32E-04	5.25E+00
38	-7.72E-04	-1.08E+01	151	4.71E-04	5.47E+00
39	-7.63E-04	-1.08E+01	152	4.79E-04	5.47E+00
40	-7.25E-04	-1.06E+01	153	4.88E-04	5.47E+00
41	-7.16E-04	-1.06E+01	154	9.36E-05	2.51E+00
42	-7.06E-04	-1.06E+01	155	1.02E-04	2.51E+00
43	-6.70E-04	-1.04E+01	156	1.10E-04	2.50E+00
44	-6.62E-04	-1.04E+01	157	1.49E-04	2.74E+00
45	-6.53E-04	-1.04E+01	158	1.59E-04	2.72E+00
46	3.77E-04	2.07E+00	159	1.69E-04	2.72E+00
47	3.84E-04	2.05E+00	160	2.07E-04	2.95E+00
48	3.91E-04	2.06E+00	161	2.16E-04	2.94E+00
49	4.32E-04	2.29E+00	162	2.24E-04	2.94E+00
50	4.40E-04	2.29E+00	163	-1.72E-04	-4.01E-02
51	4.49E-04	2.28E+00	164	-1.64E-04	-4.21E-02
52	4.90E-04	2.50E+00	165	-1.54E-04	-3.72E-02
53	4.95E-04	2.49E+00	166	-1.15E-04	1.85E-01

54	5.05E-04	2.49E+00	167	-1.06E-04	1.88E-01
55	1.09E-04	-4.66E-01	168	-9.70E-05	1.79E-01
56	1.18E-04	-4.82E-01	169	-5.92E-05	4.02E-01
57	1.26E-04	-4.82E-01	170	-5.01E-05	4.12E-01
58	1.65E-04	-2.50E-01	171	-4.10E-05	3.99E-01
59	1.75E-04	-2.52E-01	172	-4.35E-04	-2.56E+00
60	1.83E-04	-2.58E-01	173	-4.26E-04	-2.56E+00
61	2.24E-04	-2.63E-02	174	-4.16E-04	-2.56E+00
62	2.32E-04	-3.37E-02	175	-3.79E-04	-2.35E+00
63	2.41E-04	-3.27E-02	176	-3.70E-04	-2.34E+00
64	-1.55E-04	-3.01E+00	177	-3.60E-04	-2.35E+00
65	-1.47E-04	-3.02E+00	178	-3.24E-04	-2.13E+00
66	-1.39E-04	-3.02E+00	179	-3.12E-04	-2.13E+00
67	-9.90E-05	-2.80E+00	180	-3.05E-04	-2.13E+00
68	-9.05E-05	-2.80E+00	181	7.31E-04	1.03E+01
69	-8.00E-05	-2.80E+00	182	7.40E-04	1.03E+01
70	-4.52E-05	-2.57E+00	183	7.50E-04	1.03E+01
71	-3.41E-05	-2.58E+00	184	7.87E-04	1.05E+01
72	-2.55E-05	-2.58E+00	185	7.94E-04	1.05E+01
73	-4.14E-04	-5.53E+00	186	8.04E-04	1.05E+01
74	-4.03E-04	-5.54E+00	187	8.40E-04	1.07E+01
75	-3.96E-04	-5.54E+00	188	8.48E-04	1.07E+01
76	-3.58E-04	-5.31E+00	189	8.55E-04	1.07E+01
77	-3.49E-04	-5.32E+00	190	4.73E-04	7.77E+00
78	-3.41E-04	-5.33E+00	191	4.82E-04	7.77E+00
79	-3.05E-04	-5.10E+00	192	4.91E-04	7.77E+00
80	-2.95E-04	-5.10E+00	193	5.30E-04	8.00E+00
81	-2.86E-04	-5.11E+00	194	5.40E-04	7.99E+00
82	-6.68E-04	-8.04E+00	195	5.47E-04	7.98E+00
83	-6.58E-04	-8.04E+00	196	5.86E-04	8.21E+00
84	-6.49E-04	-8.04E+00	197	5.96E-04	8.21E+00
85	-6.11E-04	-7.83E+00	198	6.04E-04	8.21E+00
86	-6.03E-04	-7.83E+00	199	2.16E-04	5.27E+00
87	-5.94E-04	-7.83E+00	200	2.22E-04	5.27E+00
88	-5.57E-04	-7.60E+00	201	2.31E-04	5.26E+00
89	-5.48E-04	-7.61E+00	202	2.72E-04	5.48E+00
90	-5.39E-04	-7.61E+00	203	2.80E-04	5.48E+00
91	4.98E-04	4.81E+00	204	2.88E-04	5.47E+00
92	5.06E-04	4.80E+00	205	3.28E-04	5.70E+00
93	5.17E-04	4.81E+00	206	3.36E-04	5.70E+00
94	5.55E-04	5.04E+00	207	3.44E-04	5.69E+00
95	5.63E-04	5.03E+00	208	-4.91E-05	2.73E+00
96	5.72E-04	5.02E+00	209	-3.72E-05	2.72E+00
97	6.09E-04	5.25E+00	210	-2.90E-05	2.73E+00
98	6.19E-04	5.24E+00	211	1.02E-05	2.96E+00
99	6.29E-04	5.24E+00	212	1.90E-05	2.95E+00
100	2.35E-04	2.29E+00	213	2.76E-05	2.95E+00
101	2.45E-04	2.29E+00	214	6.53E-05	3.17E+00
102	2.53E-04	2.28E+00	215	7.45E-05	3.18E+00
103	2.93E-04	2.52E+00	216	8.29E-05	3.18E+00
104	3.02E-04	2.51E+00	217	-3.10E-04	2.02E-01
105	3.10E-04	2.50E+00	218	-3.01E-04	1.96E-01
106	3.50E-04	2.73E+00	219	-2.91E-04	1.85E-01
107	3.56E-04	2.73E+00	220	-2.52E-04	4.23E-01
108	3.67E-04	2.72E+00	221	-2.46E-04	4.09E-01
109	-3.19E-05	-2.55E-01	222	-2.34E-04	4.04E-01
110	-2.29E-05	-2.56E-01	223	-1.96E-04	6.36E-01
111	-1.44E-05	-2.63E-01	224	-1.90E-04	6.32E-01
112	2.64E-05	-2.54E-02	225	-1.81E-04	6.28E-01
113	3.08E-05	-4.20E-02			

**Appendix D. Response Values of Pitch Angle (degrees) and Pitch Rate
(degrees per second) at the Muzzle From DOE Analysis**

Run #	Pitch Angle	Pitch Rate	Run #	Pitch Angle	Pitch Rate
1	-1.21E-05	-7.92E-02	114	-1.11E-05	-6.20E-02
2	-1.13E-05	-8.30E-02	115	-6.88E-06	-6.16E-02
3	-9.18E-06	-8.24E-02	116	-6.49E-06	-6.55E-02
4	-1.25E-05	-8.10E-02	117	-6.03E-06	-6.19E-02
5	-9.32E-06	-8.94E-02	118	-1.27E-05	-5.66E-02
6	-1.34E-05	-8.24E-02	119	-1.41E-05	-6.46E-02
7	-9.71E-06	-8.56E-02	120	-1.29E-05	-6.34E-02
8	-1.16E-05	-8.55E-02	121	-1.04E-05	-6.47E-02
9	-8.33E-06	-8.39E-02	122	-1.04E-05	-6.12E-02
10	-1.53E-05	-7.26E-02	123	-1.18E-05	-6.35E-02
11	-1.01E-05	-7.25E-02	124	-1.30E-05	-6.21E-02
12	-1.26E-05	-7.50E-02	125	-1.46E-05	-6.27E-02
13	-1.53E-05	-7.90E-02	126	-1.46E-05	-5.39E-02
14	-1.13E-05	-8.17E-02	127	-2.28E-05	-7.63E-02
15	-1.30E-05	-7.94E-02	128	-1.50E-05	-7.22E-02
16	-1.25E-05	-8.35E-02	129	-2.11E-05	-7.92E-02
17	-1.39E-05	-7.97E-02	130	-2.25E-05	-7.32E-02
18	-1.38E-05	-8.15E-02	131	-1.46E-05	-7.46E-02
19	-1.63E-05	-7.16E-02	132	-1.56E-05	-7.58E-02
20	-1.86E-05	-7.29E-02	133	-1.53E-05	-7.28E-02
21	-1.36E-05	-7.02E-02	134	-2.11E-05	-7.90E-02
22	-1.46E-05	-7.19E-02	135	-1.47E-05	-7.01E-02
23	-1.91E-05	-7.82E-02	136	-4.74E-07	-3.60E-02
24	-1.35E-05	-6.95E-02	137	-8.76E-06	-4.03E-02
25	-1.53E-05	-7.38E-02	138	-2.89E-06	-3.96E-02
26	-1.40E-05	-7.35E-02	139	-3.05E-06	-4.33E-02
27	-1.88E-05	-7.50E-02	140	-7.78E-06	-4.65E-02
28	-2.51E-05	-8.93E-02	141	-1.01E-06	-4.12E-02
29	-1.92E-05	-9.98E-02	142	-1.47E-06	-4.29E-02
30	-2.54E-05	-9.57E-02	143	-7.64E-06	-4.69E-02
31	-2.07E-05	-9.36E-02	144	-3.02E-06	-4.64E-02
32	-1.95E-05	-9.56E-02	145	-7.00E-06	-5.20E-02
33	-1.92E-05	-9.87E-02	146	-5.15E-06	-4.94E-02
34	-1.77E-05	-9.25E-02	147	-2.53E-06	-5.03E-02
35	-1.86E-05	-8.90E-02	148	-8.24E-06	-4.26E-02
36	-1.78E-05	-8.78E-02	149	-8.47E-06	-5.41E-02
37	-2.46E-05	-1.07E-01	150	-4.86E-06	-4.99E-02
38	-2.58E-05	-1.05E-01	151	-5.61E-06	-5.08E-02
39	-1.95E-05	-1.05E-01	152	-5.71E-06	-5.51E-02
40	-1.91E-05	-1.02E-01	153	-4.50E-06	-5.19E-02
41	-2.53E-05	-1.12E-01	154	-1.05E-05	-6.02E-02
42	-1.92E-05	-1.09E-01	155	-8.52E-06	-5.69E-02
43	-1.95E-05	-1.09E-01	156	-5.43E-06	-5.21E-02
44	-2.08E-05	-1.10E-01	157	-4.33E-06	-5.38E-02
45	-2.29E-05	-1.07E-01	158	-8.97E-06	-5.51E-02
46	-1.14E-05	-6.06E-02	159	-5.49E-06	-5.09E-02
47	-7.31E-06	-6.80E-02	160	-3.38E-06	-5.45E-02
48	-5.15E-06	-7.87E-02	161	-5.48E-06	-5.45E-02
49	-5.25E-06	-6.94E-02	162	-5.27E-06	-5.51E-02
50	-1.12E-05	-6.32E-02	163	-1.08E-05	-5.81E-02
51	-6.91E-06	-6.81E-02	164	-1.22E-05	-5.10E-02
52	-1.39E-05	-6.95E-02	165	-1.28E-05	-5.04E-02

53	-1.03E-05	-6.71E-02	166	-6.09E-06	-4.97E-02
54	-7.34E-06	-6.64E-02	167	-1.17E-05	-5.58E-02
55	-1.02E-05	-7.18E-02	168	-9.40E-06	-5.32E-02
56	-9.10E-06	-7.06E-02	169	-9.25E-06	-5.56E-02
57	-7.89E-06	-7.32E-02	170	-1.09E-05	-4.72E-02
58	-1.36E-05	-6.64E-02	171	-6.88E-06	-4.95E-02
59	-8.63E-06	-6.57E-02	172	-1.54E-05	-5.59E-02
60	-9.65E-06	-7.92E-02	173	-1.57E-05	-6.57E-02
61	-1.13E-05	-7.50E-02	174	-1.29E-05	-6.17E-02
62	-8.89E-06	-7.69E-02	175	-1.83E-05	-5.79E-02
63	-8.28E-06	-7.48E-02	176	-1.26E-05	-6.14E-02
64	-1.61E-05	-6.48E-02	177	-1.19E-05	-6.34E-02
65	-1.19E-05	-6.54E-02	178	-1.20E-05	-5.98E-02
66	-1.33E-05	-6.03E-02	179	-1.12E-05	-6.58E-02
67	-1.29E-05	-6.20E-02	180	-9.32E-06	-6.34E-02
68	-1.24E-05	-6.85E-02	181	-5.34E-06	-2.37E-02
69	-1.12E-05	-6.89E-02	182	-2.39E-06	-2.86E-02
70	-1.25E-05	-7.18E-02	183	-5.95E-06	-2.42E-02
71	-1.09E-05	-7.52E-02	184	-6.45E-07	-3.24E-02
72	-1.00E-05	-7.20E-02	185	-6.26E-07	-3.19E-02
73	-1.96E-05	-7.20E-02	186	1.97E-07	-3.54E-02
74	-1.61E-05	-7.54E-02	187	-3.82E-07	-3.28E-02
75	-1.95E-05	-7.18E-02	188	-7.80E-07	-4.74E-02
76	-1.33E-05	-7.02E-02	189	-2.80E-06	-4.56E-02
77	-1.59E-05	-7.37E-02	190	-4.05E-06	-3.25E-02
78	-1.40E-05	-6.99E-02	191	-4.33E-06	-3.27E-02
79	-1.31E-05	-6.54E-02	192	-7.14E-06	-3.29E-02
80	-1.51E-05	-6.81E-02	193	6.35E-07	-2.40E-02
81	-1.25E-05	-6.60E-02	194	-2.54E-06	-2.77E-02
82	-2.55E-05	-1.07E-01	195	-6.23E-07	-3.53E-02
83	-1.87E-05	-9.95E-02	196	-4.77E-06	-3.26E-02
84	-1.92E-05	-9.01E-02	197	-1.85E-06	-3.14E-02
85	-1.83E-05	-9.87E-02	198	-2.93E-07	-2.65E-02
86	-1.82E-05	-9.14E-02	199	-1.96E-06	-3.34E-02
87	-1.78E-05	-9.49E-02	200	-8.28E-06	-4.58E-02
88	-2.52E-05	-9.48E-02	201	-4.06E-06	-4.13E-02
89	-1.87E-05	-9.04E-02	202	-4.05E-06	-4.16E-02
90	-1.82E-05	-8.48E-02	203	-3.78E-06	-3.60E-02
91	-9.42E-06	-6.13E-02	204	-1.04E-06	-3.47E-02
92	-9.11E-06	-5.97E-02	205	-9.63E-06	-4.21E-02
93	-4.53E-06	-6.34E-02	206	-4.54E-06	-3.72E-02
94	-1.26E-05	-6.32E-02	207	-1.37E-06	-3.84E-02
95	-5.56E-06	-6.61E-02	208	-5.64E-06	-5.00E-02
96	-4.96E-06	-6.69E-02	209	-6.43E-06	-5.68E-02
97	-1.06E-05	-6.64E-02	210	-5.28E-06	-5.19E-02
98	-8.42E-06	-5.92E-02	211	-9.93E-06	-4.99E-02
99	-4.15E-06	-6.24E-02	212	-7.29E-06	-5.51E-02
100	-1.13E-05	-5.59E-02	213	-5.39E-06	-5.80E-02
101	-6.04E-06	-5.44E-02	214	-6.79E-06	-6.13E-02
102	-5.67E-06	-5.24E-02	215	-8.51E-06	-5.59E-02
103	-5.23E-06	-5.74E-02	216	-1.10E-05	-5.28E-02
104	-1.16E-05	-5.78E-02	217	-1.45E-05	-4.03E-02
105	-6.67E-06	-5.95E-02	218	-9.35E-06	-4.49E-02
106	-5.25E-06	-5.86E-02	219	-8.91E-06	-4.44E-02
107	-8.25E-06	-5.49E-02	220	-1.20E-05	-4.21E-02
108	-7.60E-06	-6.03E-02	221	-5.03E-06	-3.99E-02
109	-8.68E-06	-6.03E-02	222	-7.11E-06	-4.58E-02
110	-1.19E-05	-6.37E-02	223	-7.51E-06	-4.79E-02
111	-7.77E-06	-5.97E-02	224	-1.25E-05	-4.84E-02
112	-8.51E-06	-6.26E-02	225	-8.90E-06	-5.29E-02
113	-1.08E-05	-6.51E-02			

Appendix E. Muzzle Yaw Rate Response Surface Model

Yaw Rate =

$$\begin{aligned} & -0.0382555 \\ & + 22.130582*m_1_DVAR1^1 \\ & + 0.0470008*m_1_DVAR1^2 \\ & -1.2546547*m_1_DVAR1^3 \\ & -0.2870402*m_1_DVAR1^4 \\ & -24.247422*m_1_DVAR2^1 \\ & + 0.7437520*m_1_DVAR2^2 \\ & + 4.3396506*m_1_DVAR2^3 \\ & -10.929489*m_1_DVAR2^4 \\ & + 4.3966138*m_1_DVAR3^1 \\ & + 0.3686572*m_1_DVAR3^2 \\ & -0.2295074*m_1_DVAR4^1 \\ & -0.2410928*m_1_DVAR4^2 \\ & -0.1858409*m_1_DVAR1^1*m_1_DVAR2^1 \\ & -9.1011244*m_1_DVAR1^1*m_1_DVAR2^2 \\ & + 3.3528814*m_1_DVAR1^1*m_1_DVAR2^3 \\ & + 102.40121*m_1_DVAR1^1*m_1_DVAR2^4 \\ & + 5.7971309*m_1_DVAR1^2*m_1_DVAR2^1 \\ & -23.345489*m_1_DVAR1^2*m_1_DVAR2^2 \\ & -142.31337*m_1_DVAR1^2*m_1_DVAR2^3 \\ & + 296.02608*m_1_DVAR1^2*m_1_DVAR2^4 \\ & + 4.6142887*m_1_DVAR1^3*m_1_DVAR2^1 \\ & + 62.316845*m_1_DVAR1^3*m_1_DVAR2^2 \\ & -88.765857*m_1_DVAR1^3*m_1_DVAR2^3 \\ & -645.38186*m_1_DVAR1^3*m_1_DVAR2^4 \\ & -31.992573*m_1_DVAR1^4*m_1_DVAR2^1 \\ & + 340.65048*m_1_DVAR1^4*m_1_DVAR2^2 \\ & + 1149.1930*m_1_DVAR1^4*m_1_DVAR2^3 \\ & -4828.8155*m_1_DVAR1^4*m_1_DVAR2^4 \\ & + 0.0101512*m_1_DVAR1^1*m_1_DVAR3^1 \\ & -2.1992555*m_1_DVAR1^1*m_1_DVAR3^2 \\ & -0.1974511*m_1_DVAR1^2*m_1_DVAR3^1 \\ & + 10.337655*m_1_DVAR1^2*m_1_DVAR3^2 \\ & + 1.6240706*m_1_DVAR1^3*m_1_DVAR3^1 \\ & + 67.437639*m_1_DVAR1^3*m_1_DVAR3^2 \\ & + 3.6905101*m_1_DVAR1^4*m_1_DVAR3^1 \\ & -81.671584*m_1_DVAR1^4*m_1_DVAR3^2 \\ & + 0.2473838*m_1_DVAR1^1*m_1_DVAR4^1 \\ & -23.019755*m_1_DVAR1^1*m_1_DVAR4^2 \\ & + 2.5622601*m_1_DVAR1^2*m_1_DVAR4^1 \\ & + 44.319995*m_1_DVAR1^2*m_1_DVAR4^2 \\ & -3.5102280*m_1_DVAR1^3*m_1_DVAR4^1 \\ & + 447.26400*m_1_DVAR1^3*m_1_DVAR4^2 \\ & -38.447680*m_1_DVAR1^4*m_1_DVAR4^1 \\ & -929.80467*m_1_DVAR1^4*m_1_DVAR4^2 \\ & + 0.0845332*m_1_DVAR2^1*m_1_DVAR3^1 \\ & + 2.5522685*m_1_DVAR2^1*m_1_DVAR3^2 \\ & + 3.5032358*m_1_DVAR2^2*m_1_DVAR3^1 \\ & -114.51127*m_1_DVAR2^2*m_1_DVAR3^2 \\ & -9.5816661*m_1_DVAR2^3*m_1_DVAR3^1 \\ & -40.971053*m_1_DVAR2^3*m_1_DVAR3^2 \\ & -86.326790*m_1_DVAR2^4*m_1_DVAR3^1 \end{aligned}$$

$$\begin{aligned} &+ 2134.0838*m_1_DVAR2^4*m_1_DVAR3^2 \\ &+ 0.5946552*m_1_DVAR2^1*m_1_DVAR4^1 \\ &-3.2714349*m_1_DVAR2^1*m_1_DVAR4^2 \\ &+ 5.7887772*m_1_DVAR2^2*m_1_DVAR4^1 \\ &-101.96563*m_1_DVAR2^2*m_1_DVAR4^2 \\ &-11.512353*m_1_DVAR2^3*m_1_DVAR4^1 \\ &-73.605912*m_1_DVAR2^3*m_1_DVAR4^2 \\ &-113.37572*m_1_DVAR2^4*m_1_DVAR4^1 \\ &+ 2464.6675*m_1_DVAR2^4*m_1_DVAR4^2 \\ &+ 0.6580689*m_1_DVAR3^1*m_1_DVAR4^1 \\ &-24.594084*m_1_DVAR3^1*m_1_DVAR4^2 \\ &+ 19.504442*m_1_DVAR3^2*m_1_DVAR4^1 \\ &+ 425.07388*m_1_DVAR3^2*m_1_DVAR4^2 \end{aligned}$$

<u>NO. OF COPIES</u>	<u>ORGANIZATION</u>	<u>NO. OF COPIES</u>	<u>ORGANIZATION</u>
1 (PDF ONLY)	DEFENSE TECHNICAL INFORMATION CTR DTIC OCA 8725 JOHN J KINGMAN RD STE 0944 FORT BELVOIR VA 22060-6218	1	ATK ORDNANCE SYS ATTN B BECKER MN07 MW44 505 LINCOLN DR EDINA MN 55436
1	US ARMY RSRCH DEV & ENGRG CMD SYSTEMS OF SYSTEMS INTEGRATION AMSRD SS T 6000 6TH ST STE 100 FORT BELVOIR VA 22060-5608	1	SCIENCE APPLICATIONS INTL CORP ATTN J NORTHRUP 8500 NORMANDEALE LAKE BLVD SUITE 1610 BLOOMINGTON MN 55437
1	DIRECTOR US ARMY RESEARCH LAB IMNE ALC IMS 2800 POWDER MILL RD ADELPHI MD 20783-1197	3	GOODRICH ACTUATION SYSTEMS ATTN T KELLY P FRANZ J CHRISTIANA 100 PANTON ROAD VERGENNES VT 05491
1	DIRECTOR US ARMY RESEARCH LAB AMSRD ARL CI OK TL 2800 POWDER MILL RD ADELPHI MD 20783-1197	2	ARROW TECH ASSOC ATTN W HATHAWAY MARK STEINOFF 1233 SHELBURNE RD STE D8 SOUTH BURLINGTON VT 05403
2	DIRECTOR US ARMY RESEARCH LAB AMSRD ARL CS OK T 2800 POWDER MILL RD ADELPHI MD 20783-1197	1	KLINE ENGINEERING CO INC ATTN R W KLINE 27 FREDON GREENDEL RD NEWTON NJ 07860-5213
1	AEROPREDICTION INC ATTN F MOORE 9449 GROVER DRIVE, STE 201 KING GEORGE VA 22485	1	GEORGIA INST TECH DEPT AEROSPACE ENGR ATTN M COSTELLO 270 FERST STREET ATLANTA GA 30332
1	UNIV OF TEXAS AT ARLINGTON MECH & AEROSPAC ENG DEPT ATTN J C DUTTON BOX 19018 500 W FIRST ST ARLINGTON TX 76019-0018	1	AIR FORCE RSRCH LAB AFRL/MNAV ATTN G ABATE 101 W EGLIN BLVD, STE 333 EGLIN AFB FL 32542-6810
2	ATK TACTICAL SYSTEMS DIV ALLEGANY BALLISTICS LAB ATTN D J LEWIS J S OWENS 210 STATE ROUTE 956 ROCKET CENTER WV 26726	1	COMMANDER US ARMY ARDEC AMSRD AAR AEM A ATTN G MALEJKO BLDG 95 PICATINNY ARSENAL NJ 07806-5000
1	ATK ADVANCED WEAPONS DIV ATTN R H DOHRN MN06-1000 5050 LINCOLN DR EDINA MN 55436	1	COMMANDER US ARMY ARDEC AMSRD AAR AEP E ATTN D CARLUCCI BLDG 94 PICATINNY ARSENAL NJ 07806-5000

NO. OF
COPIES ORGANIZATION

1 COMMANDER
 US ARMY ARDEC
 ASMRD AAR AEP E
 ATTN C KESSLER
 BLDG 3022
 PICATINNY ARSENAL NJ 07806-5000

1 COMMANDER
 US ARMY ARDEC
 ASMRD AAR AEP E
 ATTN I MEHMEDAGIC
 BLDG 94
 PICATINNY ARSENAL NJ 07806-5000

1 PM MAS
 ATTN SFAE AMO MAS
 BLDG 354
 PICATINNY ARSENAL NJ 07806-5000

3 US ARMY AMRDEC
 AMSAM RD SS AT
 ATTN R W KRETZSHMAR
 L AUMAN E VAUGHN
 REDSTONE ARSENAL AL 35898-5000

1 COMMANDER
 US ARMY ARDEC
 AMSTA DSA SA
 ATTN A CLINE
 PICATINNY ARSENAL NJ 07806-5000

4 COMMANDER
 US ARMY ARDEC
 AMSRD AAR AEM I B 65N
 ATTN J STEINER R P MAZESKI
 D J DURKIN R MONTENEGRO
 PICATINNY ARSENAL NJ 07806-5000

ABERDEEN PROVING GROUND

1 DIRECTOR
 US ARMY RSCH LABORATORY
 ATTN AMSRD ARL CI OK (TECH LIB)
 BLDG 4600

14 DIRECTOR
 US ARMY RSCH LABORATORY
 ATTN AMSRD ARL WM J SMITH
 AMSRD ARL WM B M ZOLTOSKI
 AMSRD ARL WM BC P PLOSTINS
 J NEWILL M CHEN (3 CYS)
 J DESPIRITO J SAHU
 B GUIDOS S SILTON
 P WEINACHT M BUNDY